Preliminary dosimetric characterization of EDBreast gel

Christel Stien, Alice Rousseau, jean-marc bordy, Jean Gouriou

Title:
Dosimetric characterization of EDBreast gel

Author names and affiliations:
Christel Stien[a] (corresponding author) ; christel.stien@cea.fr
Alice Rousseau[a] ; alice.rousseau@cea.fr
Jean-Marc Bordy[a] ; jean-marc.bordy@cea.fr
Jean Gouriou[a] ; jean.gouriou@cea.fr

[a]Université Paris-Saclay, CEA, List, Laboratoire National Henri Becquerel (LNE-LNHB), F-91120 Palaiseau, France.

Declaration of interest: None

Abstract:
Purpose: EDBreast gel is a new Fricke gel dosimeter, read by Magnetic Resonance Imaging, which composition includes a high amount of sucrose in order to lower diffusion effects. This paper aims at determining the dosimetric characteristics of this gel dosimeter.
Methods: This characterization has been performed in high energy photon beams. The dose-response of the gel has been evaluated as well as its detection limit, its fading effects, the reproducibility of its response, and its stability over time. Its energy and dose-rate dependence has been investigated, and the overall dose uncertainty budget established. Once characterized, the dosimetry method has been applied to a simple irradiation case, with the measurement of the lateral dose profile of a 2 x 2 cm² field of a 6 MV photon beam. The results have been compared with microDiamond measurements.
Results: EDBreast response exhibits a polynomial dose response on the 2 – 20 Gy range. It is more sensitive at low doses than the common Fricke gel dosimeters, but its sensitivity decreases with the dose enhancement, and the uncertainty of 8 % ($k = 1$) at 20 Gy is higher than the requirement of quality controls in radiotherapy. However, the gel dose profile measurements, corrected for diffusion effects, show a good agreement with the microDiamond detector results, as the gamma-index passing rates were over 94 % using 2 % and 2 mm criteria.
Conclusion: This work has characterized EDBreast gel dosimeter in an exhaustive way, and has proposed the good practices for its use.

Keywords: 3D dosimetry, Fricke-based gel dosimetry, MRI reading, dosimetric characterization

1. Introduction

The recent improvements of radiotherapy devices lead to a better targeting of the tumor thanks to the use of small radiation fields and targeting technics. However, these new treatment modalities are accompanied with novel issues concerning the reliability of dose measurements, emphasizing the need of new end-to-end quality assurance and pre-treatment controls. To respond to the needs in terms of patient specific quality assurance, an accurate 3D dosimetry with a high spatial resolution is required; gel dosimetry is a good candidate for this purpose.

There are different types of gel dosimeters, including Fricke-based gels, polymer gels, and plastic radiochromic gels. They are generally read using either Magnetic Resonance Imaging (MRI) or optical imaging [1]. Fricke-based gels contain Fe(II) ions dispersed in the gel matrix that are oxidized into Fe(III) ions under irradiation, by reaction with water radiolysis products in the presence of oxygen [2]. As Fe(III) ions are paramagnetic, the dose distribution can be measured by MRI, as the variation of Fe(III) ions concentration is related to the variation of the spin relaxation rate of hydrogen nuclei [3]. Fricke-based gels have the advantage of being non-toxic, easy to prepare, and to allow the measurement of the spatial dose distribution soon after irradiation [4], instead of polymer gels for instance. However, they face a significant problem for their use in clinics, as they are subject to ferric ion diffusion effects, with diffusion coefficients ranging between 3 10^{-10} and 5 10^{-10} m^2 s^{-1} [4–8], that infer a deformation of the dose distribution. Some improvements of the gel have been proposed to overcome these issues. The most common one is the use of an iron chelator such as Xylenol Orange or Turnbull Blue, which reduces the diffusion coefficient of the gel to less than 2.5 10^{-10} m^2 s^{-1} and 2.0 10^{-10} m^2 s^{-1} respectively [6,9,10]. However, it has been shown that the addition of chelating agents reduces the MRI sensitivity of the gel [11]. Polyvinyl alcohol has also been used as a gelling agent to reduce diffusion effects, but the high viscosity of those gels was problematic for the preparation of large volumes [12].

In order to stabilize the Fe(III) ions into the gel, Coulaud *et al*. proposed another alternative with EDBreast hydrogel, which chemical composition is intended to reduce the ferric diffusion in Fricke gel dosimeter without reducing its sensitivity by adding high amount sucrose [13,14]. Healy *et al*. already used saccharide additives in a Fricke agarose-based gel doped with Xylenol Orange, but they used much lower concentrations in order to increase the sensitivity [15]. In EDBreast gel, a diffusion coefficient of ferric ions of 3.1 10^{-10} m^2 s^{-1} has been measured [6]. It is higher than the values found in gelatin-based gels with Xylenol Orange chelator, but is still among the lowest diffusion coefficients of classical Fricke gelatin-based gel dosimeters [6]. This gel has been characterized in terms of diffusion, chemical interactions, and some of its radiological and physical properties have been determined: density ρ, mass attenuation coefficient μ/ρ, mass energy-absorption coefficient μ_{en}/ρ, mass stopping power S/ρ, and mass scattering power T/ρ [13,14]. However, its dose-response has not been studied yet in an exhaustive way.

The present work is aimed at determining the dosimetric characteristics of EDBreast gel for high energy radiotherapy purposes, and at comparing it with the other commonly used gels. The dose-response of the gel has been evaluated as well as its detection limit, its fading effects, the reproducibility of its response, and its stability over time. Its energy and dose-rate dependence has been investigated, and the overall dose uncertainty budget established.

2. Material and methods

2.1. Gel vials, irradiation and reading methods

2.1.1. Gel preparation

EDBreast gel is prepared in-house. It is composed of 7 %wt porcin gelatin (270 Bloom, Sigma-Aldrich) and 10 %wt sucrose (Sigma-Aldrich) dissolved in 40 °C water to which sulfuric acid (Fluka Analytical) and ammonium iron(II) sulfate (Fluka Analytical) are added, for final concentrations of 30 mM and 1 mM respectively. The preparation protocol has been described by Coulaud *et al*. in previous papers [13,14]. Once prepared, the gel is poured into dedicated cylindrical vials of different sizes according to the study. The gel vials are slowly cooled at room temperature (about 20 °C) and then stored in the fridge at 6 °C to complete the gelling. They are then kept at irradiation room temperature for thermal stabilization before irradiation. These gelling and thermal stabilization times depend on the volume of gel contained in the vials. For the purpose of the experiments, several series of gel vials were made out of different batches of gel and used in the following studies. The number of batches and vials used for each experiment is given in Table 1.

	$R_{2,0}$ measurement	Dose response	Energy response	Dose rate dependence	Sensitivity	Stability over time	Dose profile measurement	
							Calibration	Profile
Number of batches B / Number of vials per batch S	3 / 8	5 / 8	1 / 34	1 / 32	4 / 8	3 / 10	B = 1 Method 1: S = 10 Method 2: S = 4	S = 3
Beam energies[(1)] (MV)	-	6	6 (8), 10(8), 15 (8), 20 (8)	6	6	6	6	
Dose rates[(1)] (Gy min^{-1})	-	3.73	3.73	0.37 (2), 0.74 (6), 1.87 (6), 3.73 (6), 5.60 (6)	3.73	3.73	3.73	
Targeted dose at reference point (Gy)	-	5 – 30	20	20	20	20	2.5 – 30	16.4
Diameter / height of the vials (cm) {Volume (mL)}	2.5 / 3.5 {17}	2.5 / 3.5 {17}	1.5 / 7 {12}	2.5 / 3.5 {17}	2.5 / 3.5 {17}	2.5 / 3.5 {17}	1.5 / 7 {12}	5 / 10 {200}
ROI dimensions : edge sizes[(2)] (mm) / Number of voxels	c = 12.5 / 625	c = 12.5 / 625	c = 9 / 81	c = 13 / 169	c = 12.5 / 625	c = 12.5 / 625	Method 1: c = 9 / 324 Method 2: l = 2 ; h = 37 / 296	l = 2 ; h = 3.5 / 28
Pixel size (mm²)	0.5 x 0.5	0.5 x 0.5	1 x 1	1 x 1	0.5 x 0.5	0.5 x 0.5	0.5 x 0.5	

[(1)] corresponding number of vials are given between parenthesis
[(2)] edge size c given for squared ROI, and length l and height h given for rectangular ROI

Table 1: Specific vial, irradiation, reading and data analysis parameters of the experiments.

2.1.2. MRI readings

Readings of the irradiated gels were performed using a 1.5 T Philips Achieva MRI system (Best, The Netherlands) with a SENSE head coil. Measurements were done in terms of spin-spin relaxation time T_2. 2D maps were acquired with a single 4 mm depth slice, using a Multi-spin-echo sequence (31 echoes) with the following parameters: TR = 2000 ms, TE = 11 - 352 ms and a slice thickness of 4 mm. Pixel sizes are given in Table 1 for each experiment. R_2 is then calculated using a home-made VisualBasic program.

As the variation of relaxation rate due to irradiation, ΔR_2, depends on the absorbed dose, a non-irradiated vial made out of the same batch of gel is also read for each experiment. Thus, for a given voxel in the irradiated gel, the variation of relaxation rate is given by $\Delta R_2 = R_2 - \overline{R_{2,0}}$, with $\overline{R_{2,0}}$ the average R_2 value calculated in the voxels of a selected squared region of interest (ROI) in the non-irradiated gel. The sensitivity is, thus, defined as the ratio of the variation of the relaxation rate over the variation of the quantity to measure, which is here the absorbed dose to water D_{w} [16]:

$$S = \frac{d(\Delta R_2)}{dD_w} \quad (1)$$

That definition was used for the evaluation of the sensitivity of the response when the dose tends towards zero. The sensitivity was also used for the reproducibility, dose rate and energy response evaluations with 20 Gy irradiations. For those, we made the following approximation for simplification purpose:

$$S_{20} = \frac{\Delta R_2}{D_{\mathrm{w}}} \quad (2)$$

For the homogeneous irradiation of a gel vial s, taken from a gel batch b, R_2 values are also averaged in a squared ROI to obtain $\overline{R_{2}}_{\mathrm{b,s}}$, so that the variation of relaxation rate is given by:

$$\Delta R_{2\,b,s} = \overline{R_{2}}_{b,s} - \overline{R_{2,0}}_{b} \quad (3)$$

with $\overline{R_{2,0}}_{\mathrm{b}}$ the average of the $\overline{R_{2,0}}$ values obtained in the non-irradiated gel vials over the whole batch b.

2.1.3. Specific irradiation and reading conditions for the studies

For the dose and energy responses, the stability and the reproducibility studies, the gel was poured into cylindrical vials of different sizes (Table 1). Considering the gel volumes used for these studies, half an hour was sufficient for gelling, and 3.5 h for thermal stabilization before irradiations. Irradiations were done between 4 h and 7 h after preparation. They were undertaken on the Laboratoire National Henri Becquerel (LNE-LNHB) TrueBeam linear accelerator (Varian Medical Systems, Palo Alto, CA), with 6, 10, 15 and 20 MV photon beams, under the TRS 398 reference conditions [17]. Thus, the vials were placed one by one in a water tank of 30 x 30 x 30 cm^3, their geometrical center at 10 cm depth and their longitudinal axis perpendicular to the beam axis. The absorbed dose to water values are directly traceable to the French national references based on calorimetry primary measurements [18]. Readings were performed within the 5 hours after irradiation (except for the stability study), and the gel vials have been transported from the irradiation device to the reading one in a thermally controlled cooling box at 20 °C. As gels were uniformly irradiated for the characterization studies, the diffusion effects were not considered, unlike profile measurements. The variation of the beam profile within the volume of the vials has been taken into account in the uncertainty budget. The profile measurements required more specific preparation, irradiation and reading conditions. They are described in more details in Section 2.2.4. Table 1 summarizes the irradiation, reading and data analysis parameters for each experiment, as well as the size of the vials used for each experiment. These vials are also shown in Figure 1 (a).

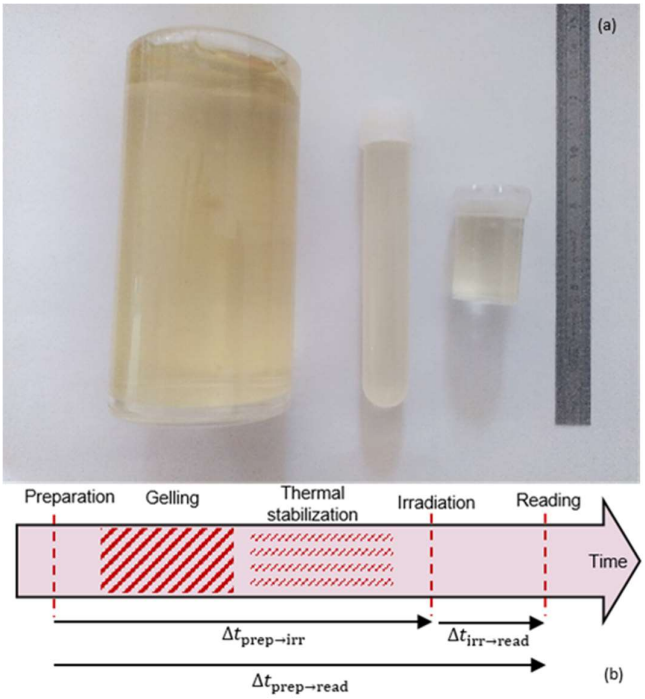

Figure 1: (a) Gel vials used for the experiments and (b) time scale of the preparation, irradiation, and reading of the gel.

2.2. Methods for dosimetric characteristics evaluation

2.2.1. Reproducibility of $R_{2,0}$ measurement and of sensitivity

The reproducibility of both $R_{2,0}$ measurement and sensitivity have been assessed at several levels:

- the uniformity within the voxels of a given ROI in a gel vial *s*,
- the distribution of the results of the *S* gel vials prepared from a given batch *b*, named hereafter "partial reproducibility",
- the overall reproducibility over *B* batches.

2.2.2. Dose and energy responses and dose-rate dependence studies

The gel has been studied in terms of dose-rate, energy and dose responses as described in Table 1. The parameters of the dose-response functions, $D = f(\overline{\Delta R_2})$, have been determined using the Levenberg-Marquardt algorithm of OriginPro software (OriginLab Corporation), with their associated standard deviations and covariance terms. These calibration curves have been used for the evaluation of the dose resolution, and Minimum Detectable Dose (MDD). The concept of dose resolution, ${D_\Delta}^p$, introduced by Baldock *et al.*, is the minimum difference between two absorbed doses that can be distinguished with a specified level of confidence p [19]. It can be expressed as:

$$ {D_\Delta}^p = k_\mathrm{p} \sqrt{2}\, u(D) \qquad (4) $$

Hence, considering a 95% confidence interval and an infinite number of Gaussian distributed data points, $k_\mathrm{p} = 1.960$ and:

$$ {D_\Delta}^{95\%} = 2.77\, u(D) \qquad (5) $$

Then, using this equation (5), the MDD is given by the dose resolution when the dose approaches zero.

For the dose-rate and energy dependence studies, all gel vials were prepared from the same batch of gel. The irradiations of the dose-rate study were performed in the range 0.37 – 5.60 Gy min^{-1} and the energy dependence has been studied in photon beams between 6 MV and 20 MV (Table 1). In accordance with external radiotherapy practices, the sensitivity of the gel has been evaluated as a function of the Tissue Phantom Ratio (TPR_{20-10}) for the energy dependence evaluation.

2.2.3. Stability over time

The stability over time of the sensitivity of the gel was studied with gel irradiations and readings undertaken over 5 days. Two vials per batch were irradiated every day, starting the first irradiations 4 hours after their preparation. Every day d, the 30 gel vials (irradiated and non-irradiated ones left) were read within the 2 hours after the irradiation serie. The relaxation rate was averaged in the selected ROI to obtain $\overline{R_2}_{\mathrm{d,b,s}}$ in a vial s of a batch b for irradiated vials, and $\overline{R_{2,0}}_{\mathrm{d,b,s}}$ for non-irradiated vials. Thus, for each vial measured on day d, the variation of relaxation rate $\Delta R_{2\,\mathrm{d,b,s}}$ is obtained using equation (3), so that $\Delta R_{2\,\mathrm{d,b,s}} = \overline{R_2}_{\mathrm{d,b,s}} - \overline{R_{2,0}}_{\mathrm{d,b}}$, where $\overline{R_{2,0}}_{\mathrm{d,b}}$ is the mean $\overline{R_{2,0}}_{\mathrm{d,b,s}}$ value for batch b.
The stability of the gel was assessed regarding three parameters (Figure 1 (b)):

- Evolution of $R_{2,0}$ with the elapsed time between preparation and reading, $\Delta t_{\mathrm{prep}\rightarrow\mathrm{read}}$. This analysis took into account all of the non-irradiated gels read every day.
- Evolution of the $\Delta R_{2\,\mathrm{b,s}}$ measured in a vial, with the time between irradiation and reading $\Delta t_{\mathrm{irr}\rightarrow\mathrm{read}}$ (with $\Delta t_{\mathrm{prep}\rightarrow\mathrm{irr}}$ = 4 h), which was evaluated with the vials irradiated the first day ($d = 1$) and their reading over 4 days (this includes 2 vials for batches 1 and 3, and 1 vial for batch 2).
- Stability of the sensitivity after the preparation of the gel with the time between preparation and irradiation, $\Delta t_{\mathrm{prep}\rightarrow\mathrm{irr}}$ (considering the readings of the gel vial done just after its irradiation, so that $\Delta t_{\mathrm{irr}\rightarrow\mathrm{read}} < 2$ h). Results are given in terms of sensitivity at irradiation dose of the vial, $S_{20_{\mathrm{b,s}}}(\Delta t_{\mathrm{prep}\rightarrow\mathrm{irr}}) = {\Delta R_{2_{\mathrm{b,s}}}(\Delta t_{\mathrm{prep}\rightarrow\mathrm{irr}})}\big/{D_{\mathrm{b,s}}}$.

2.2.4. Dose profile measurements

Irradiations in simple conditions in a water tank and static squared beams are used to evaluate the accuracy of inhomogeneous dose distribution measurements using EDBreast gel. We considered the 6 MV beam with a 2 x 2 cm² field, as this field size is small enough to be representative of stereotactic measurements. Profiles are measured at reference depth into water with a cylindrical vial filled with EDBreast gel dosimeter (Table 1 and Figure 1 (a)), and with the microDiamond detector 60019 (PTW, Freiburg). This microDiamond is well suited for small field measurements and was, therefore, considered as the golden standard detector for this experiment [20].

The batch of gel was prepared one day before irradiation. It was filled in vials of two sizes: 12 small calibration vials and 8 larger flasks. Both vials and flasks were kept 5 hours in the fridge for gelling completion and left overnight in irradiation room for thermal stabilization.

2.2.4.1. Calibration methods

Calibration was done in terms of absorbed dose to water using two methods: one based on the irradiation of a set of calibration vials (Method 1), and another one using percentage depth dose (PDD) measurements in the flasks (Method 2). For both methods, irradiations were performed in the 6 MV photon beam, under reference conditions, with a 10 x 10 cm² irradiation field. Method 1 implied the homogeneous irradiation of 10 calibration vials, while two were kept unirradiated. Method 2 was based on the measurement of 4 PDDs using 5 gel flasks (one unirradiated). The signal measured at a given depth z into the gel flask, $\Delta R_2(z)$, is related to $D_{\mathrm{w}_{\mathrm{ref}}}(z)$, the corresponding dose at the same depth measured with the microDiamond detector. This detector is calibrated against the LNE-LNHB absorbed dose to water reference:

$$D_{w_{ref}}(z) = \frac{M_{MD}(z)}{M_{MD}(z_{ref})} \times D_{w_{gel}}(z_{ref}) \quad (6)$$

with $M_{\mathrm{MD}}(z)$ and $M_{\mathrm{MD}}(z_{\mathrm{ref}})$, the signal measured with the microDiamond respectively at depth z and at reference depth z_{ref}, and $D_{\mathrm{w}_{\mathrm{gel}}}(z_{\mathrm{ref}})$ the dose calculated at reference depth for the gel measurement. It is assumed that the calibration coefficient of the microDiamond detector does not vary with depth.

Four flasks were irradiated, targeting absorbed doses to water of 2.5 Gy, 7.0 Gy, 14.0 Gy, and 25.0 Gy at the reference depth z_{ref} of 10 g cm^{-2}. The flask center was placed at reference point with the longitudinal axis along the beam direction.
All calibration irradiations and readings were done the same day, with a maximum elapsed time between irradiation and reading of 6 h for calibration vials, and 2.5 h for PDD measurements. R_2 values were averaged in squared ROI for the vials, and in rectangular ones for the flasks (Table 1). Those last ones are 4 voxels large along the axis of the flask, so that the resolution is representative of the size of the sensitive volume of the microDiamond (2 mm diameter), and they are 74 voxels high in the direction perpendicular to the axis. In these ROI, irradiations were considered as homogeneous, as the variation of lateral profile was included in the uncertainty budget. For each flask, a ΔR_2 distribution was, therefore, obtained in the relative depth range $\Delta z = z - z_{ref}$ of [-5.0 ; +5.0] g cm^{-2}, with z the depth of the voxel into the water tank, with steps of 0.2 g cm^{-2}. The ΔR_2 values were then interpolated in order to fit with the microDiamond measurements, which were done in the same Δz range with steps of 0.5 g cm^{-2}.

Monte Carlo simulations of the experiment led with Method 2 were also undertaken in order to compare the energy spectra at the entrance and at the end of the gel flask (Δz of respectively -4.9 g cm^{-2} and 4.3 g cm^{-2}) with the spectra at the same depths when the water tank is only filled with water. The BEAMnrc code was used to simulate the TrueBeam 6 MV photon beam for a 10 x 10 cm^2 field size and generated the corresponding phase-space data files at the entrance of the water phantom (phsp) [21]. The Monte Carlo model of the LNE-LNHB accelerator head is based on the information privately provided by Varian.

The photon and electron fluence spectra were calculated using the EGSnrc Monte Carlo user-code FLURZnrc [22] and the 6 MV phsp files set with an uncertainty on the average electron and photon energies of 0.1%. Two modelling geometries were studied. One consisted of a gel flask located into a water tank and the second consisted only of a single water tank. For each configuration, the detection volumes are located along the central axis of the incident beam. Each detector has a cylindrical shape with a radius of 0.5 cm and a thickness of 0.07 cm. The characteristics of the water material at the reference temperature of 20 °C were obtained from the water ICRU-90 density correction file, included

in the EGSnrc Monte Carlo code distribution. The elemental composition of the gel used for the simulations is given in Table 2. It has to be noted that the composition of the gelatin is not known precisely, but assessed using the approximate proportion of the main amino acids.

Element	Weight percentage (%)
C	7.17
H	10.39
O	81.17
Fe	0.0044
N	1.10
S	0.17

Table 1: Elemental composition of the gel considered for the Monte Carlo calculation.

2.2.4.2. Profile measurements

The microDiamond measurements were undertaken in the range [-15 ; +15] mm around z_{ref} with a 0.5 mm step. Gel dose distribution measurements were performed the same day as the calibration ones. Three profiles were acquired, using the three flasks left placed one by one into the beam in the same position as for PDD measurements, with a target dose of 16 Gy at reference point. MRI readings were performed between 1.5 h and 2.5 h after irradiation, with a single slice, placed in the radial plane, at the reference depth of 10 g cm^{-2}. Rectangular ROI were selected with 4 voxels along the profile axis to fit with the size of the sensitive volume of the microDiamond detector and 7 voxels along the horizontal axis. R_2 values were averaged, and corrected for the blank measured in the unirradiated flask to get the distribution of ΔR_2. The dose distributions $D(x)$ were obtained using the calibration curves previously established, and were then normalized to the central point, $D_{\mathrm{n}}(x) = D(x)/D(x=0)$, for the comparison with the microDiamond results. To compare the penumbras and Full Widths at Half Maximum (FWHM), profiles were fitted with a sigmoid function:

$$D_{n,fit}(x) = A \times \frac{1}{1 + e^{-\lambda \times (x - x_0)}} + B \qquad (7)$$

where A, B, λ and x_0 are the fitting parameters, x_0 being representive of the inflexion point.

To take into account the time between irradiation and reading, gel profiles have been corrected for diffusion effects, considering a diffusion coefficient of 3.1 ± 0.1 10^{-10} m² s^{-1} measured by Coulaud *et al.* for the EDBreast gel (average value obtained with the 4 methods presented in the paper) [6]. For this correction, it was considered that diffusion over a time t was monodirectional for each side of the profile, and that it occurred in a semi-infinite medium. Profiles have been fitted with a complementary error function:

$$D(x,t) = \frac{(D_{max} - D_{min})}{2} \times Erfc\left(\frac{x - x_0}{\sigma(t) \times \sqrt{2}}\right) + D_{min} \qquad (8)$$

where $\sigma^2(t) = 2\, d_{\mathrm{Fe}} \times t$

with $D_{\max}$ and $D_{\min}$ the maximum and minium doses measured respectively, d_{Fe} the diffusion coefficient, and $\sigma(t)$ the standard deviation of the complementary error function.

This standard deviation at irradiation time $\sigma(t_{\mathrm{irr}})$ can be calculated to estimate the initial signal profile:

$$\sigma^2(t_{\mathrm{irr}}) = \sigma^2(t_{\mathrm{lect}}) - 2\, d_{\mathrm{Fe}} \times (\Delta t_{\mathrm{irr}\to\mathrm{lect}}) \quad (9)$$

In addition, a global gamma-index analysis was conducted using the *Pymedphys* library in Python (0.37.1) with passing criteria of (0.5%/0.5mm), (1%/1mm), (2%/2mm) and (3%/3mm) [23]. The microDiamond values were considered as the reference distribution and a linear interpolation function of gel dose distribution values was used.

3. Results

3.1. Reproducibility of $R_{2,0}$ measurement

The uniformity of measurement of $R_{2,0}$, within the volume of the ROI, between the voxels v in a vial s from a batch b, $u_{\mathrm{v}}(R_{2,0})$, has been considered as the standard deviation of the distribution of $R_{2,0}$ among the voxels of the selected ROI, $\sigma({R_{2,0}}_{\mathrm{b,s,v}})$. The relative results are presented in Table 3 for all vials. They are ranging between 0.92 % and 1.27 %. To avoid underestimating the uncertainty budget, one considers the worst case, so that $u_{\mathrm{v}}(R_{2,0}) = 1.27\ \%$.

Number of the vial	$\sigma({R_{2,0}}_{\mathrm{b,s,v}})$ %		
	Batch 1	Batch 2	Batch 3
1	0.92	1.03	1.02
2	0.95	1.10	1.13
3	1.03	0.97	1.15
4	1.09	0.97	0.97
5	0.95	1.12	1.07
6	1.14	1.03	1.10
7	0.99	0.92	1.14
8	**1.27**	1.19	1.13

Table 2: Standard deviation of the distribution of ${R_{2,0}}_{b,s,v}$ in the voxels v of the vials s of each batch b for the determination of the uniformity over the volume of the ROI.

Two methods can be used to quantify the uncertainty on the partial reproducibility for the vials of a batch b, $u_{\mathrm{s}}(R_{2,0})$: (i) considering the mean values of the $R_{2,0}$ obtained in the voxels of the ROI selected in the vials, $\overline{{R_{2,0}}_{\mathrm{b,s}}}$, and the standard deviation of their distribution, $\sigma(\overline{{R_{2,0}}_{\mathrm{b,s}}})$, or (ii) considering all the $R_{2,0}$ measured in the voxels of batch b, regardless of the vial, through the standard deviation of their distribution, $\sigma({R_{2,0}}_{\mathrm{b,v}})$. The choice of the method is based on the analysis of the shapes of the density distributions of $R_{2,0}$ values measured in the voxels, all together or vial by vial. As shown on Figure 2 (a), for batch 3, the distributions of $R_{2,0}$ taken vial by vial display Gaussian distributions. However, they do not overlap completely for a given batch b, while the distribution of all the voxels of b considered together results in a Gaussian distribution (Figure 2 (b)). Hence, it seems more relevant to consider $u_{\mathrm{s}}(R_{2,0}) = \sigma({R_{2,0}}_{\mathrm{b,v}}) = 1.45\ \%$ (Table 4). However, if one considers the practical case of the measurement of the mean $R_{2,0}$ in a single non-irradiated vial for the determination of ΔR_2 in an irradiated gel prepared from the same batch, using $\sigma(\overline{{R_{2,0}}_{\mathrm{b,s}}})$ would be more convenient. It is here of 1.37 %. Therefore, in this experiment, the impact on the final uncertainty budget of using one method or the other is not significant, as the values considered for both cases are close.

		Batch 1	Batch 2	Batch 3
Partial reproducibility (%)	$\sigma(\overline{R_{2,0}}_{\mathrm{b,s}})$	1.37	0.69	1.03
	$\sigma(R_{2,0_{\mathrm{b,v}}})$	1.13	1.19	1.45
Overall reproducibility (%)	$\sigma(\overline{R_{2,0}}_{\mathrm{s}})$	**1.37**		
	$\sigma(R_{2,0_{\mathrm{v}}})$	**1.74**		

Table 3: Standard deviation of the distribution of $R_{2,0}$ measured in the voxels, considered all together ($\sigma(R_{2,0_{b,v}})$ and $\sigma(R_{2,0_{v}})$) or vial by vial ($\sigma(\overline{R_{2,0}}_{b,s})$ and $\sigma(\overline{R_{2,0}}_{s})$), for the determination of the partial and overall reproducibility

The same analysis is done for the evaluation of the overall reproducibility $u_{\mathrm{b}}(R_{2,0})$. With only 3 batches, the comparison of the mean $\overline{R_{2,0}}_{\mathrm{b,s}}$ values obtained for the vials of batch b, $\overline{R_{2,0}}_{\mathrm{b}}$, is meaningless. Moreover, the comparison of the $\overline{R_{2,0}}_{\mathrm{b,s}}$ for all vials, given in Figure 3, clearly shows discrepancies between the 3 batches. Considering the vial approach by using the standard deviation of the distribution of all the $\overline{R_{2,0}}_{\mathrm{b,s}}$ values obtained in the vials for all batches, $\sigma(\overline{R_{2,0}}_{\mathrm{s}})$, seems to minimize the uncertainty that could be assigned to the overall reproducibility. On the other hand, considering the voxel approach, with the standard deviation of $R_{2,0}$ values obtained in all of the voxels of all the 3 batches, $\sigma(R_{2,0_{\mathrm{v}}})$, appears to be more representative of it, and also presents a Gaussian distribution (Figure 2 (c) and 2 (d)). As a result, one considers $u_{\mathrm{b}}(R_{2,0}) = \sigma(R_{2,0_{\mathrm{v}}}) = 1.74$ % (Table 4), which is, for instance, lower than the inter-batch reproducibility of 3.1 % reported by Bero *et al*. for non-irradiated Fricke Xylenol Orange gel [24].

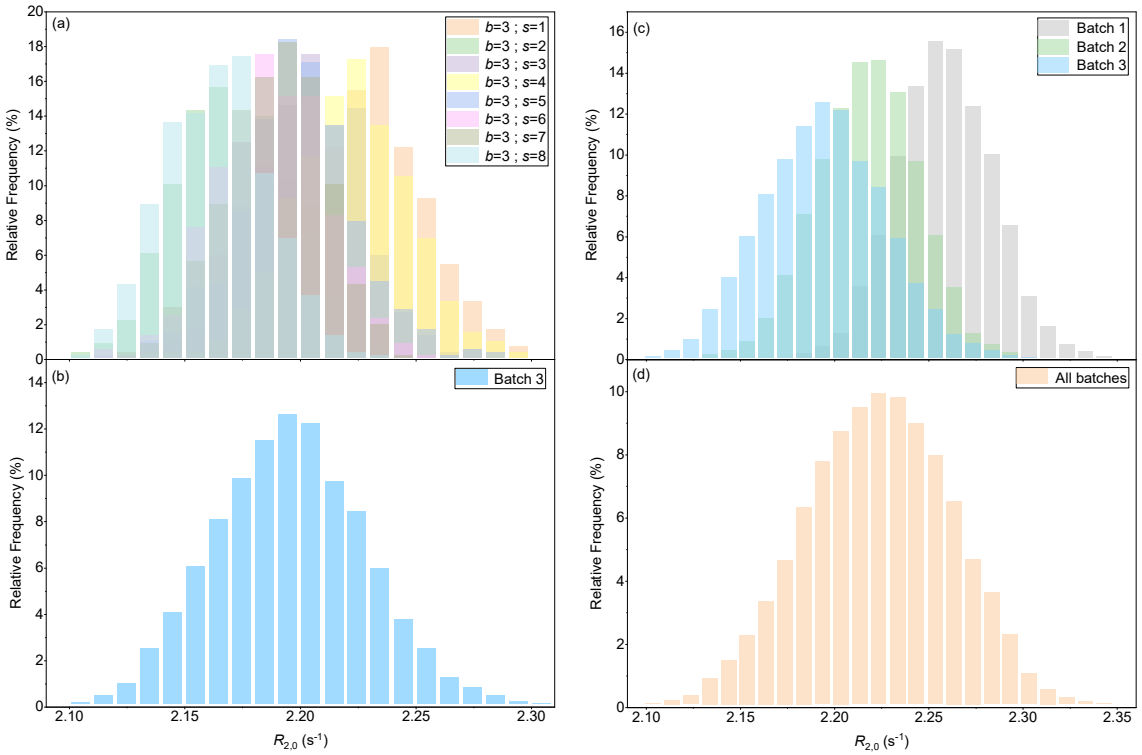

Figure 2: Distribution of $\boldsymbol{R_{2,0}}$values measured, for the partial reproducibility, in the voxels of batch 3 (a) considered vial by vial, (b) considered all together, and for the overall reproducibility, in the voxels of all the 3 batches considered (c) batch by batch, (d) all together.

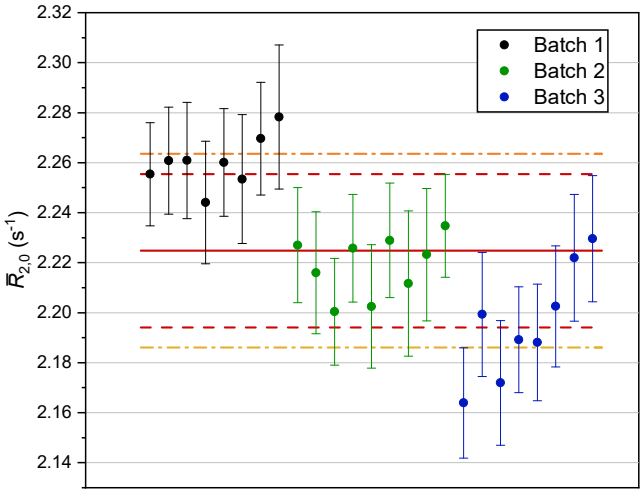

Figure 3: $\overline{\boldsymbol{R_{2,0_{b,s}}}}$ of all the vials of the 3 batches. Uncertainty bars correspond to $\boldsymbol{\sigma}(\overline{\boldsymbol{R_{2,0_{b,s}}}})$. The red plain line indicates their average value, with the dotted lines representing its associated uncertainty when considered as $\boldsymbol{\sigma}(\boldsymbol{R_{2,0_s}})$ in red, and as $\boldsymbol{\sigma}(\boldsymbol{R_{2,0_v}})$ in orange.

3.2. Dose response

The variation of relaxation rate measured in the gel vials as a function of the absorbed dose to water are plotted on Figure 4 (a) for the 5 batches. The uncertainties on $\Delta R_{2_{b,s}}$ are considered as the combination of the standard deviation of the distribution of R_2 in the irradiated vial $\sigma(R_{2_{b,s}})$ and the uncertainty on $R_{2,0}$ in the non-irradiated one, $u(R_{2,0})$, so that:

$$u(R_{2,0}) = \sqrt{\sigma(R_{2,0})^2 + u_s(R_{2,0})^2} \quad (10)$$

and $u(\Delta R_{2_{b,s}}) = \sqrt{\sigma(R_{2_{b,s}})^2 + u(R_{2,0})^2}$

with $\sigma(R_{2,0})$ the standard deviation of the distribution of $R_{2,0}$ values in the non-irradiated gel, and $u_s(R_{2,0}) = 1.37$ % the partial reproducibility considering the conclusions of Section 3.1.

The curves show a non-linear relationship, whereas most of the authors who use Fricke gels report a linear relation in the dose range investigated here [7,12,25–28]. This is however consistent with Healy *et al.*'s work, who obtained a linear relation for doses up to 10 Gy, which becomes non-linear when considering the dose range 0 – 50 Gy [15]. They attribute this behavior to the depletion of dissolved oxygen and ferrous ions, which would be accelerated by the higher radiochemical yield with the addition of 2 g L^{-1} sucrose [15,24]. As the sucrose concentration is much higher here, reaching 108 g L^{-1} in order to limit the diffusion of ferric ions, this assumption is even more relevant for EDBreast dosimetric gel, and could explain the non-linear relation.

Here, the relation between the absorbed dose to water and ΔR_2 can be fitted with a second order polynomial function,

$$D_w = a \times \Delta R_2^2 + b \times \Delta R_2 + c \quad (11)$$

The uncertainty is calculated with the law of propagation of uncertainties as [29]:

$$u(D_w) = \sqrt{\begin{array}{c}\left(\frac{\partial D_w}{\partial \Delta R_2}\right)^2 \times u(\Delta R_2)^2 + \left(\frac{\partial D_w}{\partial a}\right)^2 \times u(a)^2 + \left(\frac{\partial D_w}{\partial b}\right)^2 \times u(b)^2 + \left(\frac{\partial D_w}{\partial c}\right)^2 \times u(c)^2 \\ +2\left(\left(\frac{\partial D_w}{\partial a}\right) \times \left(\frac{\partial D_w}{\partial b}\right) \times u(a;b) + \left(\frac{\partial D_w}{\partial a}\right) \times \left(\frac{\partial D_w}{\partial c}\right) \times u(a;c) + \left(\frac{\partial D_w}{\partial c}\right) \times \left(\frac{\partial D_w}{\partial b}\right) \times u(c;b)\right)\end{array}} \quad (12)$$

with:

$$\frac{\partial D_w}{\partial a} = \Delta R_2{}^2, \qquad \frac{\partial D_w}{\partial \Delta R_2} = 2a \times \Delta R_2 + b,$$

$$\frac{\partial D_w}{\partial b} = \Delta R_2, \qquad \frac{\partial D_w}{\partial c} = 1,$$

and where $u(a;b)$, $u(a;c)$ and $u(c;b)$ are the covariance terms between the parameters a, b and c.

The relative standard uncertainty for the irradiated vials of batch 1, $u(D_{b=1,s})/D_{b=1,s}$, is given on Figure 4 (b). It leads to uncertainties of about 7 % (k=1) at 20 Gy. The contribution of the calibration curve to the final uncertainty is, thus, significant, as the uncertainty on $\Delta R_{2\,b=1,s}$ at 20 Gy is of about 1.6 %.

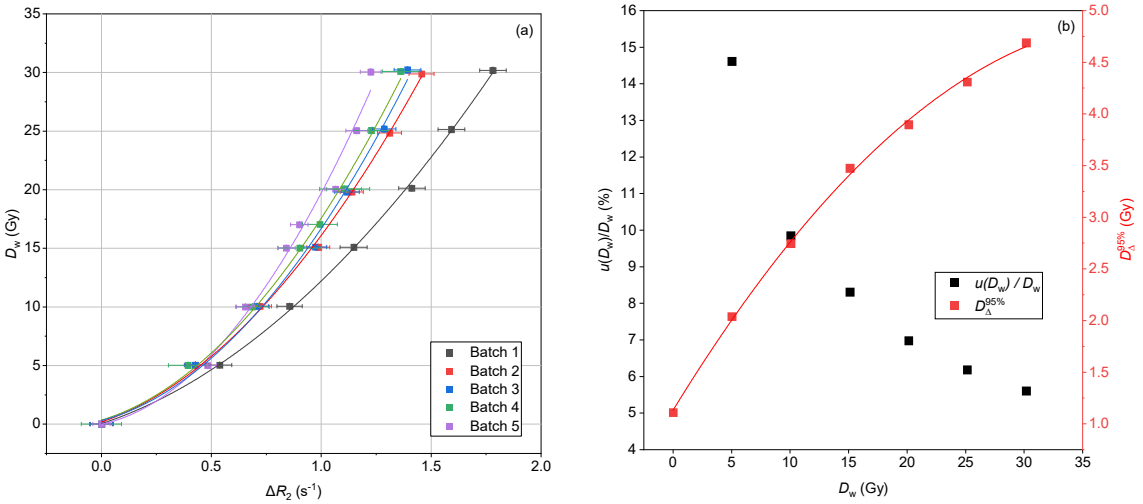

Figure 4: (a) Calibration curves established with 5 batches of gels in a 6 MV photon beam in reference conditions. The lines represent the polynomial regressions. (b) Variation of the relative standard uncertainty $\boldsymbol{u(D_w)/D_w}$ and of the dose resolution $\boldsymbol{D_\Delta{}^{95\%}(D_w)}$ with the absorbed dose to water for batch 1.

For the 5 batches, the calibration curves do not overlap, with respect to the standard deviations. To compare the calibration curves, three parameters, derived from equation (11), have been considered and compared in Figure 5. c values, which are the intercept of the regressions curves, are in accordance for all 5 batches and are also compatible with the condition $D(\Delta R_2 = 0) = 0$. Taking into account the definition given by equation (1), the sensitivity of the gel for $D(\Delta R_2) = 0$, S_0, is derived from the calibration function, and is given by $S_0 = 1/b$. For all batches, the values of S_0 are in good agreement, with a mean value of 0.178 ± 0.024 s^{-1} Gy^{-1} (standard deviation of the 5 values). The sensitivity of EDBreast for low doses (when D tends towards zero), is among the highest ones found in the literature, which were comprised between 0.015 s^{-1} Gy^{-1} and 0.13 s^{-1} Gy^{-1} [7,8,12,15,25–28]. Some authors have shown that the addition of organic material such as sucrose enhanced the sensitivity of the gel, due to chain reactions implying organic material for the production of Fe(III) ions [15]. That is the case, for example, for Hill *et al*. with PVA, with a 25 % enhancement (2 g L^{-1}) [28] and also Healy *et al*. who observed an enhancement of 122 % with their 2 g L^{-1} sucrose [15]. The sensitivity S_0 obtained here is

close to the values published by Schulz *et al*. and by Healy *et al*. (0.13 s^{-1} Gy^{-1} and 0.83 s^{-1} Gy^{-1} respectively), who also found a non-linear relationship of the dose-response [8]. Due to this polynomial response, even if the sensitivity for low doses is higher than most of Fricke gels, it decreases with the increase of the dose. For a parameter, the values are also compatible, except for batch 1. This parameter characterizes the non-linearity of the response. Indeed, $\partial^2 D / \partial \Delta {R_2}^2 = 2 \times a$ describes the linear variation of the slope of the curve with the absorbed dose, so that the more a is high, the more the slope increases rapidly with the absorbed dose, and thus, the more the saturation effects appear for low doses. The comparison of those 3 parameters shows that the response of the gel appears to be reproducible for low doses, but the saturation effects, that occur when the dose delivered increases, differ from a preparation to another, and so does the sensitivity of the gel.

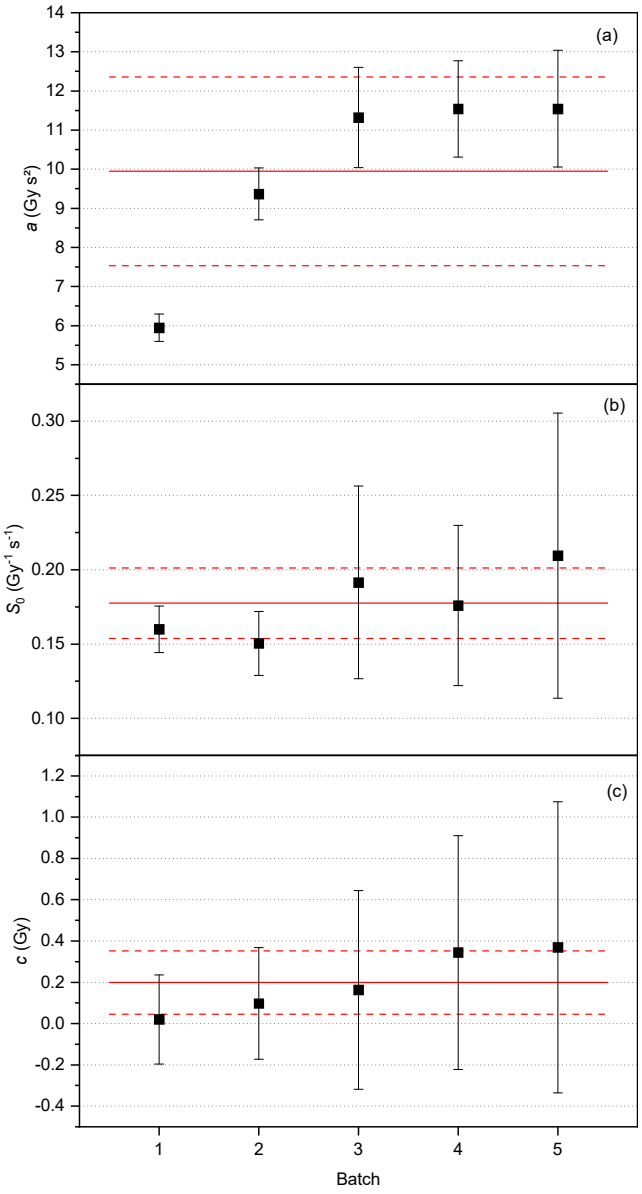

Figure 5: Comparison of the parameters of the fitting function (a) $\boldsymbol{a}$, (b) $\boldsymbol{S_0}$, and (c) $\boldsymbol{c}$ for five gel preparations.

3.3. Dose rate and energy dependence

Regarding the beam quality, the sensitivity of the gel appears to decrease when the TPR_{20-10} increases (Figure 6 (a)). A discrepancy of 3.8 % has been measured for TPR_{20-10} values between 0.66 and 0.79. Even if this variation does not seem to be large, it can be noted that it is higher than the variation of correction factors k_{Q,Q_0} for a large panel of ionization chambers. This factor corrects the response of a dosimeter for the beam quality Q to a reference beam quality Q_0 (generally between 2.3 % and 2.6 %) [17]. On the other hand, the irradiations of the gels at different dose rates do not enlighten a dependence of the response to this parameter, taking into account the uncertainties, as seen on Figure 6 (b).

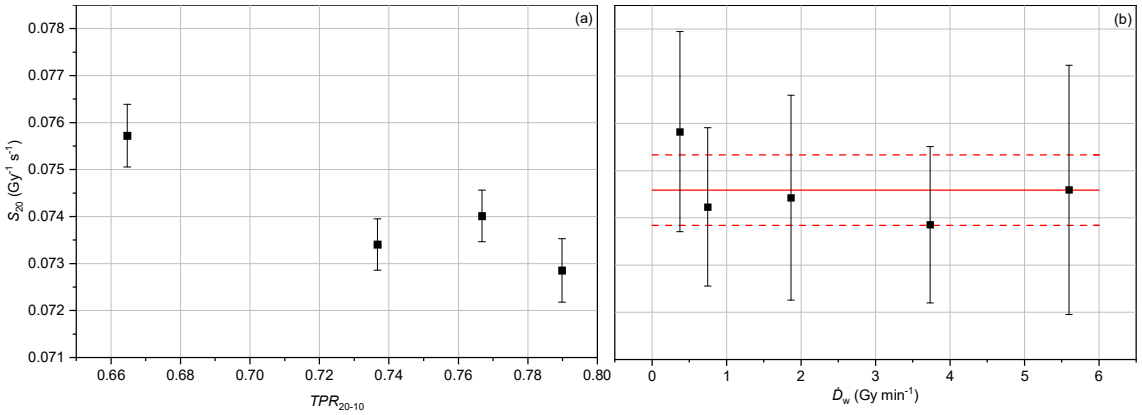

Figure 6: Variation of the sensitivity at 20 Gy, $\boldsymbol{S_{20}}$, (a) with the beam quality, represented by the $\boldsymbol{TPR_{20-10}}$, and (b) with the dose rate $\boldsymbol{\dot{D}_w}$. The plain line represents the mean value and the dashed ones, the standard deviation.

3.4. Reproducibility of the sensitivity

The lack of reproducibility of the dose-response observed in Section 3.2 also appears when studying the sensitivity with 20 Gy irradiations of series of vials from 4 different batches. The analysis of the results was done by plotting the distributions of S_{20} values obtained in the voxels of the vials, as it was done previously in Section 3.1. Figure 7 shows the dispersion of the $\overline{S_{20}}_{b,s}$ for the 4 batches. The associated uncertainty is $u\left(\overline{S_{20}}_{b,s}\right) = \sqrt{u(\Delta R_2{}_{b,s})^2 + u(D_{b,s})^2}$. It varies from 3.6 % to 5.7 % (Table 5).

Number of the vial	$u(\overline{S_{20}}_{b,s})$ (%)			
	Batch 1	Batch 2	Batch 3	Batch 4
1	4.53	5.70	4.92	4.59
2	5.39	5.05	5.21	3.63
3	5.05	5.10	3.92	4.16
4	4.16	5.21	5.14	3.92
5	5.28	5.44	3.96	3.92
6	4.59	5.32	4.24	4.23
7	4.55	5.58	4.61	4.36

Table 4: Standard uncertainties on $S_{20\,b,s}$ in the voxels v of the vials s of each batch b

The distribution of S_{20} values obtained within the ROI of a vial appears to be a Gaussian, but the discrepancies between the vial distributions are wide (Figure 8 (a) and (b)). Even considering all the voxels of all the vials of a batch, S_{20} values are not normally distributed, and neither are they when one considers all the batches together (Figure 8 (c) and (d)). So the results of this experiment do not enable the characterization of the partial and neither does it for the overall reproducibility of the sensitivity of the gel for a 20 Gy irradiation as in Section 3.1 for $R_{2,0}$. However, the vial and batch selections used here may not be sufficient, and more data could enlighten us on the behavior of the sensitivity.

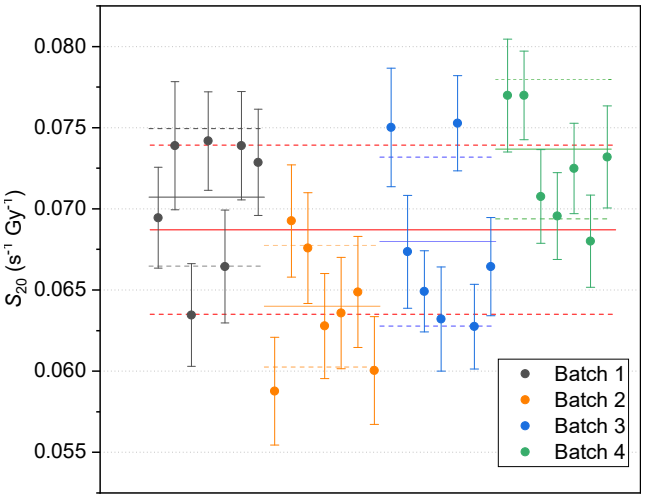

Figure 7: Comparison of the $\overline{\boldsymbol{S_{20_{b,s}}}}$ for the 4 batches. For each batch, the corresponding plain line represents the mean value of the vials of this batch, $\overline{\boldsymbol{S_{20_b}}}$, with the dotted line as the standard deviation of their distribution, $\boldsymbol{\sigma}(\overline{\boldsymbol{S_{20_b}}})$. The main plain line represents the mean value of the vials of all batches, $\overline{\boldsymbol{S_{20_s}}}$ with the dotted line as their standard deviation $\boldsymbol{\sigma}(\overline{\boldsymbol{S_{20_s}}})$.

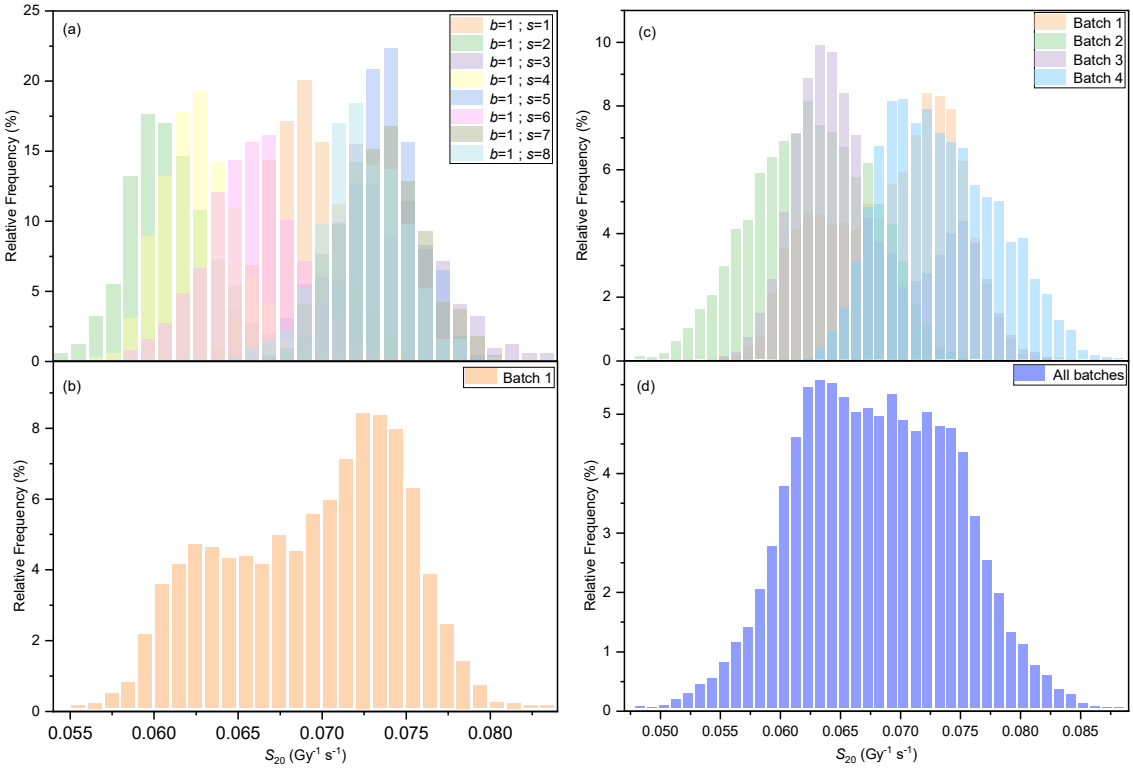

Figure 8: Distribution of $\boldsymbol{S_{20}}$ values measured in the voxels of batch 1 (a) considered vial by vial, (b) considered all together, and in the voxels of the 4 batches (c) considered batch by batch, (d) considered all together.

Even though the reproducibility cannot be determined, it can still be noted that the standard deviation of the distribution of $\overline{S_{20}}_{\mathrm{b,s}}$ within a batch, $\sigma(\overline{S_{20}}_{\mathrm{b,s}})$, is close to the standard deviation of the distribution of all S_{20} values in this batch, $\sigma(S_{20_{\mathrm{b,v}}})$, which is of about 7 %. This value is higher than the inter-sample reproducibility value reported by Bero *et al.*, which was of 3.4 % for 10 Gy irradiated gels [30]. Regarding the values of sensitivities measured in all of the 3 batches, the standard deviation of all the S_{20} taken together, $\sigma(S_{20_{\mathrm{v}}})$, is here smaller than the standard deviation of the mean values of the vials, $\sigma(\overline{S_{20}}_{\mathrm{s}})$, which is of about 7 % (Table 6).

	Batch 1	Batch 2	Batch 3	Batch 4
$\sigma(\overline{S_{20}}_{\mathrm{b,s}})$ (%)	6.04	5.92	7.73	5.89
$\sigma(S_{20_{\mathrm{b,v}}})$ (%)	6.28	6.42	7.94	5.47
$\sigma(\overline{S_{20}}_{\mathrm{s}})$ (%)	**7.58**			
$\sigma(S_{20_{\mathrm{v}}})$ (%)	**5.71**			

Table 5: Standard deviations on S_{20} obtained in the voxels, considered all together ($\sigma(S_{20_{b,v}})$ and $\sigma(S_{20_{v}})$) or vial by vial ($\sigma(\overline{S_{20}}_{b,s}$) and $\sigma(\overline{S_{20}}_{s})$), for the determination of the partial reproducibility and standard deviation over all of the 3 batches.

3.5. Dose resolution and Minimum Detectable Dose

In this study, the relative dose resolution $D_\Delta{}^{95\%}$ is not equal to the relative R_2 resolution, as proposed by De Deene *et al*., because the dose-response is not linear and $u(D)$ is not a constant (equation (12)) [31]. The MDD is, thus, obtained by fitting the curve $D_\Delta{}^{95\%} = f(D_w)$ with a second order polynomial fit.

Figure 4 (b) gives $D_\Delta{}^{95\%}$ as a function of the absorbed dose to water, taking batch 1 as an example. As expected, $D_\Delta{}^{95\%}$ tends to increase with the dose. The MDD values are between 1.12 Gy and 1.52 Gy for the batches from 1 to 3, and reach 2.31 Gy and 2.04 Gy respectively for batches 4 and 5 as the signal-to-noise ratio was higher for these ones. This method has been largely used for characterizing and comparing polymer gel dosimeters [32–36] and some authors also used it for Fricke gel dosimeters analysis [7,37–39]. They reported $D_\Delta{}^{95\%}$ values, for low irradiation doses, smaller than those obtained with EDBreast gel (Table 7), except for the optical reading methods which are more precise for low doses. Using ICRU 1972 method, which considers the MDD as the dose which increases the signal by an amount of three times the standard deviation of the unirradiated value, Olsson *et al*. also found a lower MDD of 1 Gy and 0.6 Gy respectively for gelatin and agarose-based Fricke gels [40,41]. The variation of $D_\Delta{}^{95\%}$ suggests that the gel is more suitable for "low" doses, in the limits of the MDD. However, this result should be considered in view of the relative uncertainties on the absorbed dose measured. While $D_\Delta{}^{95\%}$ increases with the absorbed dose, the relative uncertainty decreases on the dose range considered, reaching 7 % for a 20 Gy irradiation. This dosimetric gel is therefore interesting for measuring the dose delivered to the tumor and, as the optimum measurement dose has to be a compromise between obtaining a good dose resolution without getting a relative uncertainty on the absorbed dose measured too high, its performances would be at their best for doses to the tumor volume in the range 5 – 15 Gy.

Authors	Gel	Reading method	Beam quality	$D_\Delta{}^{95\%}$
Saur *et al*., 2005 [7]	Gelatin 10 %wt Fe^{2+} 1.0 mM pH 1.5	MRI, 8 echo MSE, echo spacing TE = 35 ms, TR = 345 ms, 4 repetitions	6 MV photons (Elekta Synergy)	1.5 Gy (dose range 0 – 40 Gy)
Cho *et al.*, 2013 [37]	Agarose 1 %wt, Fe^{2+} 1.0 mM, NaCl 1.0 mM, H_2SO_4 50 mM	MRI, 3D FSE: TR 600 ms, echo train length ETL 16, effective TE eTE 8.2 ms	GammaKnife (Elekta) 1.125 MeV (^{60}Co sources)	0.87 Gy at 5 Gy 3.74 Gy at 40 Gy
Viti *et al*. 2006 [38]	Agarose 1 %wt, XO 0.25 mM, Fe^{2+} 1 mM, NaCl 1 mM, H_2SO_4 50 mM	Optical tomography (567 nm)	^{60}Co and ^{137}Cs sources	0.2 Gy (dose range 0 – 3 Gy)
Rousseau *et al*. 2022 [39]	Gelatin 5 %wt XO 0.09 mM Fe^{2+} 0.3 mM pH 1.6	Optical tomography (590 nm)	6 MV photons (Varian TrueBeam)	0.056 Gy at 0.5 Gy 0.15 Gy at 4 Gy

Table 6: Dose resolutions reported for several Fricke gels in the literature.

3.6. Stability over time

3.6.1. Stability over time of the relaxation rate of the non-irradiated gel $R_{2,0} = f(\Delta t_{\text{prep}\rightarrow\text{irr}})$

The distribution of $\overline{R_{2,0}}_{\text{d,b}}$ values, obtained by averaging all the $\overline{R_{2,0}}_{\text{d,b,s}}$ of the vials s of the batch b measured on day d, has been plotted versus the elapsed time between preparation and reading, $\Delta t_{\text{prep}\rightarrow\text{read}}$ (Figure 9 (a)). For a given day d, all the measurements could not be done at once, there was an elapsed time $\Delta t_{\text{read}_{\text{d,b}}}$ that could reach 1.5 h between the first and the last measurement. Thus, the average $\overline{\Delta t}_{\text{prep}\rightarrow\text{read}_{\text{d,b}}}$ was considered for each day d and for each batch of gel b with its uncertainty $u\left(\overline{\Delta t}_{\text{prep}\rightarrow\text{read}_{\text{d,b}}}\right) = {\Delta t_{\text{read}_{\text{d,b}}}}/{2}$. Results showed that the signal increases of about 20 % after 1 day, and 50 % after 3 days, due to the spontaneous oxidation of Fe(III) ions [42,43]. Comparatively to other Fricke gel dosimeters, this enhancement is high. Kelly *et al*. reported an increase of the signal of 0.21 % per day for Fricke Xylenol Orange gel, Olsson *et al.* an increase estimated between 0.3 % and 1.2 %, and Chu *et al.* reported 2.7 % enhancement in 24 h for Fricke PVA gel [9,12,40]. Our value is however consistent with the one found by Bero *et al*., who reported an enhancement of 24 % per day for gelatin-based Fricke gel doped with benzoic acid (FBXG) [44] and with Healy *et al*.'s work, who have already observed that the addition of sucrose enhanced the spontaneous oxidation of Fe(II) of 50 % [15]. The relationship of $\overline{R_{2,0}}$ versus time seems to be quite reproducible from a preparation to another for vials of the same shape and could be fitted with a polynomial function, which would enable the establishment of a correction factor for auto-oxidation. However, these variations are intended to be very dependent on the reproducibility of preparation conditions and on the volume of the gel, particularly with the potential interactions between the outside air and the gel. Such correction may, therefore, lead to errors in the estimation of the dose.

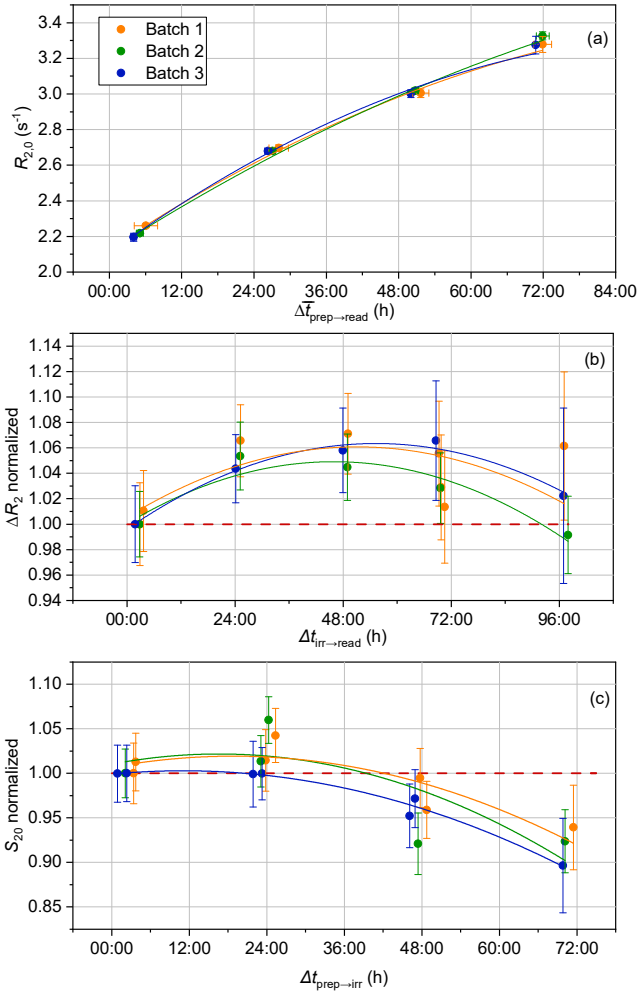

Figure 9: (a) Variation of the $\overline{\boldsymbol{R_{2,0}}}_{\mathbf{d,b}}$ of non-irradiated vials from the 3 batches over the time between preparation and reading $\overline{\boldsymbol{\Delta t}}_{\mathbf{prep\rightarrow read}}$. (b) Variation of $\boldsymbol{\Delta R_{2_{b,s}}}$ for one vial from each of the 3 batches over time after irradiation $\boldsymbol{\Delta t_{irr\rightarrow read}}$. (c) Variation of the sensitivity of the gel, $\boldsymbol{S_{20}}$, normalized to the value of the first measurement, over the time after its preparation $\boldsymbol{\Delta t_{prep\rightarrow irr}}$. Uncertainty bars respectively display $\boldsymbol{\sigma}(\overline{\boldsymbol{R_{2,0}}}_{\mathbf{d,b}})$, $\boldsymbol{\sigma}(\boldsymbol{\Delta R_{2_{b,s}}})$ and $\boldsymbol{u}(\boldsymbol{S_{20_{b,s}}})$.

3.6.2. Stability over time of the variation of relaxation rate measured on irradiated gel ($\Delta R_2 = f(\Delta t_{\mathrm{irr}\rightarrow\mathrm{read}})$)

To ensure the stability over time of the response of the gel, this auto-oxidation phenomenon has to follow the same behavior on non-irradiated vials and on irradiated ones, respectively for $R_{2,0}$ and for R_2 measurements, in order to offset each other. It has been shown that the composition of the gel, and particularly the Fe(II) ions concentration, largely affects its post-irradiation stability [42,45]. Figure 9 (b) plots $\Delta R_{2_{\mathrm{b,s}}}$ normalized to the value of the first reading versus $\Delta t_{\mathrm{irr}\rightarrow\mathrm{read}}$. The curves $\Delta R_{2_{\mathrm{b,s}}} = f(\Delta t_{\mathrm{irr}\rightarrow\mathrm{read}})$ over 4 days show an increase up to 7 % for about 2 days after irradiation and then decrease, certainly due to the aging of the gel (gel matrix stability, drying of the gel over time, etc.). Therefore, the auto-oxidation occurring in the non-irradiated vial, for $R_{2,0}$ measurement, does not compensate the one occurring in the irradiated one. While $u\left(\Delta R_{2_{\mathrm{d,b,s}}}\right)$ ranges here from 3 % to 6 %,

these variations cannot be neglected. It was already recommended to read the dosimeters soon after irradiation, due to diffusion issues, but the instability of ΔR_2 over the time after irradiation emphasizes this recommendation, and extends it to the homogeneously irradiated vials, such as the ones used for the establishment of the calibration curve.

3.6.3. Stability over time of the sensitivity ($S_{20} = \Delta t_{\mathrm{prep}\rightarrow\mathrm{irr}}$)

The variation of the sensitivity over time is representative of the variation of the radiochemical yield. Figure 9 (c) shows, for each batch b studied, the distribution of $S_{20_{\mathrm{b,s}}}$ normalized to the value of the first vial irradiated versus $\Delta t_{\mathrm{prep}\rightarrow\mathrm{irr}}$. After a slight increase of about 2 % one day after preparation, the sensitivity of the gel tends to decrease of about 5 % in two days, and 8 % in three days.
Schulz *et al*. observed, for Fricke agarose-based gel, that the initial slope of the calibration curve was 40 % higher than two days later, while Bero *et al*. reported a variation of 5 % in 24 h with the FBXG gel [8,44,46].

The stability of the system over time depends on the concentration of ferrous ions, as the rate of this process is proportional to the square of the concentration of ferrous ions [45]. Thus, the phenomenon could be reduced by lowering this concentration, but this would lead to a decrease of the sensitivity [46]. Also, a low acidity would stabilize the system, while increasing it would lower the sensitivity.

3.7. Dose distribution measurements

3.7.1. Calibration curve and volume effects

The calibration curves obtained with both calibration vials (Method 1) and PDD (Method 2) methods show a good agreement, within the limits of the uncertainties, for doses up to 10 Gy (Figure 10). For doses above 17 Gy, the curves tend to diverge, as the difference between the doses for a given ΔR_2 is bigger than the uncertainty (> 8 %). One might consider that the perturbation of the water medium with the gel, more pronounced with Method 2 than with Method 1, might be responsible for this discrepancy.

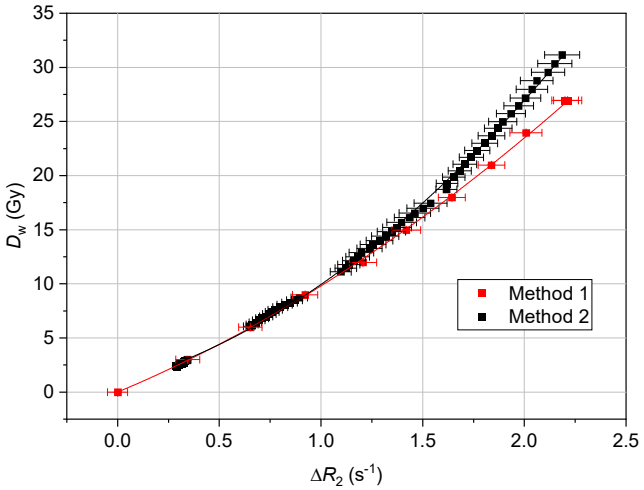

Figure 10: Calibration curves obtained using the vials irradiated under reference conditions (Method 1) and using PDD measurements (Method 2). Uncertainty bars represent the standard deviation of $\boldsymbol{\Delta R_2}$ distribution in the corresponding ROI. For Method 2, each group of points corresponds to one PDD vial.

Figure 11 shows the photon energy spectra, calculated using Monte Carlo simulations for Method 2 on one hand and replacing the gel by water on a second hand (reference conditions for absorbed dose to water measurement). The photon spectra shapes are very close for the two different geometries, except for a peak at approximately 6.4 keV due to the K band of fluorescence of the iron contained in the gel. In order to qualitatively estimate the differences between the photon spectra for the two different studied geometries, the corresponding absorbed doses were determined for each position. The maximum difference observed between the absorbed doses for the same position does not exceed 0.6 % to be compared with a statistical uncertainty of about 0.15 %, which shows that the perturbation of the medium by the dosimeter is very small. Also, as the energy spectra are different at the entrance and at the end of the dosimeter, one could attribute the difference between both methods to a potential energy dependence of the calibration factor, but such case would imply that the calibration curve with Method 2 using the central point of each gel flasks would be similar to the curve established with Method 1 at the same depth, which is not the case. Therefore, the discrepancy between the calibration curves cannot be explained by the perturbation of the medium by the gel, neither by a potential energy dependence of the sensitivity of the gel, especially considering the results of the study described in Section 3.2, but is more likely explained by volume effects.

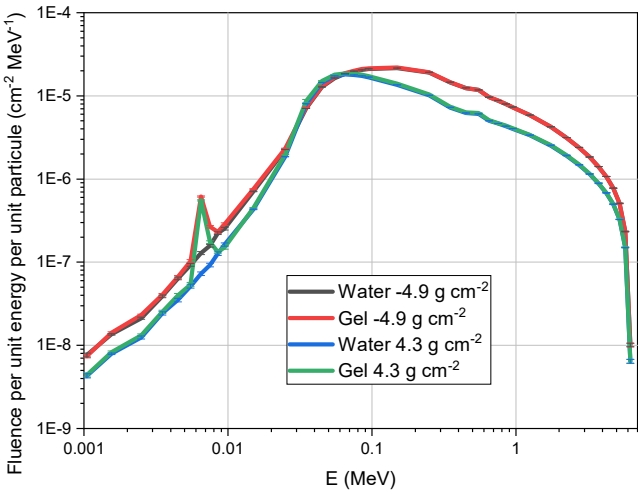

Figure 11: Energy spectra obtained by Monte Carlo simulations at the entrance and at the end of the PDD measurement gel flask, and at the same depth with the tank filled with water.

Indeed, the sensitivity of the gel may vary with the volume analyzed. Volume effects have been reported by several authors for gel dosimeters using MRI reading [3,31,47]. For BANG gels, MacDougall *et al*. observed, in non-irradiated vials, a higher transverse relaxation rate for large volumes than for small ones. They also showed that the sensitivity of the gel increases with the volume of the vial irradiated [48]. Olsson *et al*. have shown, for Fricke agarose-based gels, that the sensitivity varies with the cooling rate of the gel [26]. These volume effects are attributed to the "gel temperature history", and more specifically the cooling rate, as it varies with the volume of the vial, and thus induces a non-uniform O_2 distribution within the gel [27,31,48,49]. However, Healy *et al*. have shown that the addition of sucrose, and more broadly non-gelling polysaccharides, could eliminate the cooling rate dependence of the gel, yet with a smaller concentration than ours [15].

Hence, it is recommended to establish the calibration curve using the same volumes of gel as the one of the vial irradiated for the experiment, in order to avoid volume effects. Indeed, the deviations that are due to those volume effects are not reproducible, and, thus, cannot be corrected for [31]. To overcome

these effects and avoid the need to establish a calibration curve with different vials, some authors recommend the use of radiosensitive gels as relative dosimeters, with a dose distribution that would be renormalized to a reference point and calibrated either using an external, more reliable, "golden standard", such as TLD, or ionization chamber [3,31,50] or the dose value calculated by the TPS at that point [49]. This implies, however, to work with the gel in a linear dose range which is not the case here. If the dose-response cannot be considered as linear, the establishment of a calibration curve remains, thus, mandatory. This can be done easily for the study of small gel volumes, of the same order as the calibration vials (in the limits of the appearance of artifacts due to small volumes), but is more complicated for large volumes. For these, some authors established the calibration curve with the irradiation at different calibration doses into the zones not irradiated with the patient treatment plan [51–53]. However, that would lead to irradiating these zones out of reference conditions, and using TPS calculated doses as reference ones, while it is intended to be validated by absolute dosimetry. Therefore, Method 2 would be a good alternative, with the PDD measured with the same batch of gel and calibrated with a golden standard. This method was also used for calibrating gel dosimeters in terms of dose or energy dependence by several authors [51,54–56].

In order to assess their accuracy, both calibration methods were applied for the calculation of the dose at the reference point taken on the beam axis for the three lateral dose profiles measured with the gel. The absorbed dose to water calculated using the monitor chamber and corrected for the beam output was considered as the reference value. It was 16.09 ± 0.07 Gy. The average dose value with Method 1 is 18.3 Gy, while it is 17.1 Gy with Method 2. For both cases, the uncertainty on the dose measured calculated using equation (12) was 7 %, and the maximum dose difference between the 3 experiments was 1.7 %. Method 1 is, therefore, compatible with the reference value, unlike Method 2, contrarily to what was expected. These discrepancies have not been explained yet and emphasize the fact that absolute dosimetry using Fricke gel dosimeter with MRI reading is hard to manage. Given these results, Method 1 has been used for calibrating the lateral dose profile measured, as it provides the most accurate results at reference point.

3.7.2. Profile measurements

The three normalized dose profiles were measured along the vertical axis (Ox). They are plotted on Figure 12 (a) together with the profile measured with the microDiamond detector. The overall uncertainty on the dose, calculated as previously described, is of 8 % ($k = 1$) on the beam axis. The dose distributions obtained with the gels are quite reproducible for the three experiments, but they show variations in the high doses region, where the dose distribution was intended to be flatter. Yet, these variations are of the same order of magnitude as the uniformity previously estimated into the volume of a larger ROI (Table 6).

The distributions $D_{\mathrm{n}}(\mathrm{x})$ obtained with both types of dosimeters show large differences, with penumbral widths about 1.5 mm higher for gel dosimeters than for the microDiamond, while the steps of the profile was only of 0.5 mm. However, the FWHM are in good agreement with a difference of less than 0.25 mm.

The profiles corrected for diffusion effects are plotted on Figure 12 (b). Figure 12 (c) presents the dose corrected profile averaged over the 3 gel dosimeters along with the distribution of relative uncertainties, $u(D_{\mathrm{n}})/D_{\mathrm{n}}$, and relative dose differences between gel and microDiamond measurements $\Delta D_{\mathrm{n}}/D_{\mathrm{n}}$. The uncertainty on the diffusion coefficient has an impact on the FWHM lower than 0.02 mm, and lower than 0.2 mm on penumbra regions. The standard deviation on the determination of the inflexion point,

x_0, is of about 0.04 mm with both sigmoid and error fitting functions (equations (7) and (8) respectively for the determination of the FWHM and diffusion coefficient). The corrected profiles present a better match with the microDiamond results. However, this correction enhanced the discrepancy between the profiles in the out-of-field areas. The difference between the penumbra widths measured with both dosimetric methods is less than 0.5 mm, which is the same order of magnitude as the step of the profile. The FWHM is however larger than expected considering the microDiamond results, as they show a difference between 0.95 mm and 1.35 mm. Profile measurements have been performed at several depths with the microDiamond to evaluate the impact of the uncertainty of the position of the MRI slice into the gel (0.8 mm) and of its depth (4 mm). However, this uncertainty has only been estimated at 0.3 mm, which does not explain the gap between the gel and the microDiamond FWHM. Nevertheless, for all the positions with doses over the MDD, the difference between the dose measured by gel and with the microDiamond is lower than the uncertainty.

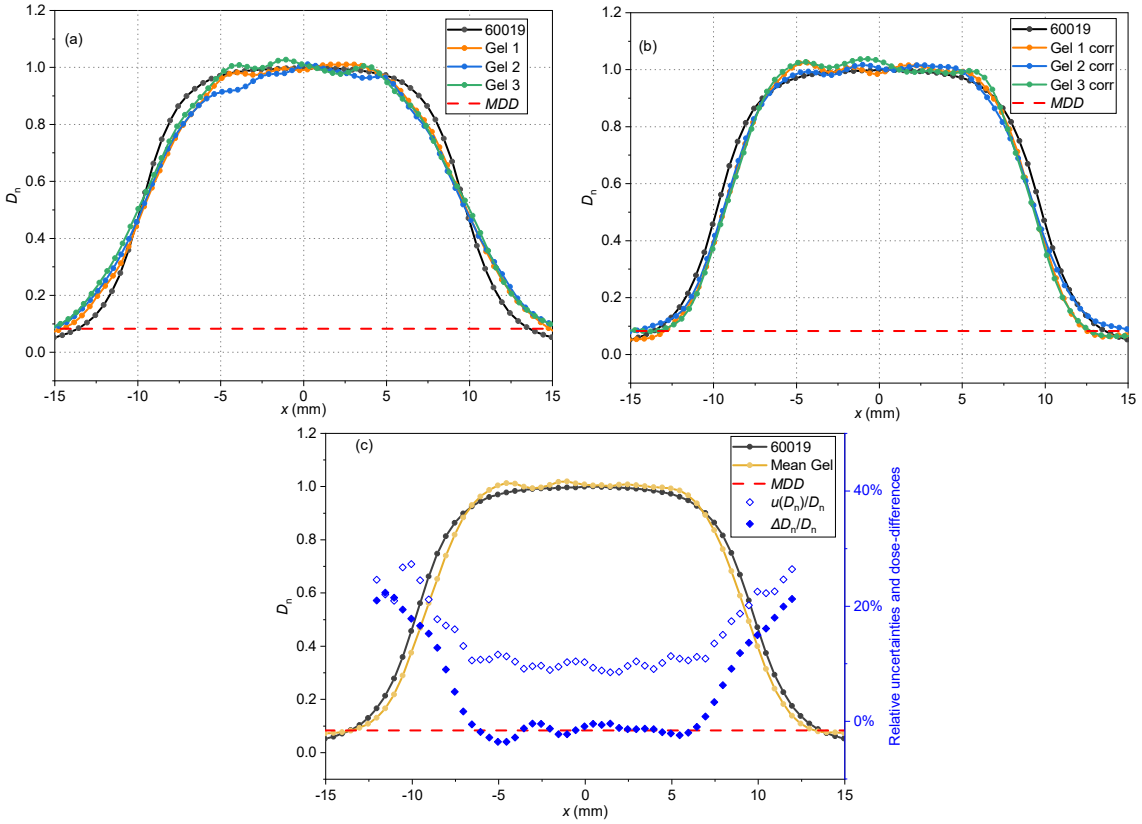

Figure 12: Lateral dose profiles normalized to central point (a) uncorrected and (b) corrected for diffusion effects for three gel dosimeters and for the microDiamond detector, and (c) averaged corrected profile with the relative uncertainties and dose differences.

For the gamma-index analysis, the values lower than 15 % of the maximum dose were not taken into account, considering the MDD. Passing rates are given in Table 8

Table 7 for the three gel profiles. Results are lower than 64 % for the three experiments with (0.5%/0.5mm) criterion, but are higher than 85 % for two of them with (1%/1mm) criterion (the third profile being less accurate on the plateau), and higher than 92 % whatever the experiment with dose and distance criteria over (2%/2mm).

	Uncorrected profiles		Diffusion correction		Gamma-index passing rates (%)			
	$\Delta(Penumbra)$ (mm)	$\Delta(FWHM)$ (mm)	$\Delta(Penumbra)$ (mm)	$\Delta(FWHM)$ (mm)	(0.5%/0.5mm)	(1%/1mm)	(2%/2mm)	(3%/3 mm)
Gel 1	1.64	0.24	0.26	0.95	41	88	100	100
Gel 2	1.93	0.04	0.22	1.15	63	88	100	100
Gel 3	1.85	0.19	0.51	1.35	35	69	94	100

Table 7: Comparison results between gel and microDiamond profiles. Penumbra and FWHM differences, respectively written Δ(Penumbra) *and* Δ(FWHM) *and gamma-index passing rates.*

4. Discussion

This work has been conducted in order to characterize EDBreast dosimetry gel for its application in high energy photon beams. This Fricke gelatin-based gel, read by MRI, has the particularity of containing a high concentration of sucrose, which purpose is to limit diffusion effects of ferric ions. The addition of sucrose, or other non-gelling polysaccharides, into a gelatin-based Fricke gel had already been done by Healy *et al*. for enhancing the sensitivity (2 g L^{-1}). They enlightened that the presence of this additive impacts several other dosimetric properties, such as the dose linearity, the spontaneous oxidation of Fe(II) ions, and the cooling rate dependence [15]. EDBreast gel, with its sucrose concentration even higher, presents dosimetric characteristics that are consistent with this work. Its response is non-linear on the dose range 0 – 30 Gy and it is one of the most sensitive Fricke gels associated to MRI readings found in the literature for low doses, but also one of the most affected by spontaneous oxidation of ferrous ions. However, while Healy's work showed that polysaccharide could limit volume effects, it was not the case here, with the sucrose concentration used.
These parameters have to be taken into account for the dosimetry protocol, in order to avoid potential errors on the measurement of the dose, or an increase of the uncertainties. Considering the stability over time of the response, due to the spontaneous oxidation of ferrous ions, the blank correction has to be performed with a gel made out of the same preparation as the irradiated ones, and read at the same time. The sensitivity of the gel is at its highest 2 days after its preparation. Also, even if it was known that, for dose gradient measurements, readings have to be performed soon after irradiation due to diffusion effects, this is also the case for gels homogeneously irradiated, as the signal is not stable over time.

With its polynomial dose-response behavior, the sensitivity and dose resolution of the gel are higher for low doses than for high ones, and the reproducibility of the response is good for doses up to 10 Gy, where saturation effects are the less pronounced. The variations of sensitivities from a preparation to another obtained for upper doses are, indeed, higher than those found in the literature (7 %).
The establishment of a calibration curve with gel vials made out of the same batch of gel and with similar shape and size as the studied one is, thus, mandatory. Its contribution to the uncertainty budget is, however, significant (7 % at k = 1). Also considering the volume and partial reproducibility of the response of the gel, irradiated or not, the overall uncertainty on a dose measured in the range 10 – 20 Gy is of about 8 % (k = 1). Therefore, as the relative uncertainty tends to decrease with the dose, the MDD is about 2 Gy and considering the sensitivity and the reproducibility of the response, the optimal dose-range found here for the use of EDBreast is 5 – 15 Gy.

Based on this characterization, the dose profile measurements were performed to evaluate the suitability of the method for assessing the dose distribution delivered by a small field of size 2 x 2 cm^2. Even though, the PDD calibration method (Method 2) was expected to be the most suitable method to avoid volume effects, the irradiation of small calibration vials was found to be more accurate. The three

relative dose profiles measured with the gel are reproducible between each other, but they show discrepancies with the profile measured with a microDiamond detector, considered as the reference one. Correcting gel profiles for diffusion effects improved the results in the penumbra regions, but the discrepancy appearing between the FWHM shows the complexity of using diffusion effects correction for determining the "true" dose distribution. For the dose gradient considered here, the increase of the standard deviation of the complementary error function, $\Delta\sigma$, is given in Table 9 for several amounts of time. With the pixel size of 0,5 mm used in our measurements, differences of profiles are visible 45 min after irradiation. As the maximum time between irradiation and reading is 2.5 h, a pixel size of 1.5 mm would be more appropriate. This is consistent with the gamma-index passing rates obtained, which show a good match from (2%/2mm) criteria.

$\Delta\sigma$ (mm)	0.5	1.0	1.5	2.0	2.5	3.0
Δt	45 min	1 h 45	3 h	4 h 30	6 h	8 h

Table 8: Increase of the standard deviation of the complementary error function, $\Delta\sigma$, for different elapsed times between irradiation and reading.

To verify if a 3D dosimetry system meets the stringent requirement for radiotherapy applications, Oldham *et al*. proposed the RTAP criteria (Resolution-Time-Accuracy-Precision), which is defined by maximum 1 mm^3 spatial resolution and 1 hour imaging time, accuracy to within 3% and precision within less than 1% [57]. In accordance with Oldham *et al*'s work, the accuracy is considered as the uncertainty on the dose measured, and the precision as the volume reproducibility. With its 1.5 mm spatial resolution, 30 min scanning time, 7 % accuracy, and 5.7 % precision, the method used in this study does not meet the ideal RTAP criteria (1 mm, 60 min, 3 %, 1 %), as many of the Fricke gel dosimeters read using MRI [57–59], but it keeps the advantage over them of a lower diffusion coefficient than classical Fricke gels, and a higher sensitivity than Fricke gels doped with chelators. Those last gels associated to optical readings remain more accurate than the gel dosimetry method studied here, nevertheless MRI readings keep being an interesting tool, as it presents the capability of analyzing a wider panel of vial shapes. However, EDBreast gel dosimeter is still less performant than PVA Fricke hydrogels, that combine an enhancement of the sensitivity with the limitation of diffusion effects [60,61]. Also, the non-linearity of the response hinders its use as a relative dosimeter without establishing a calibration curve, thus enhancing the uncertainties. Some work could be done to improve the linearity, as Coulaud suggested with preparing the gel under an oxygen flow [62].

5. Conclusion

The dosimetric characterization, in high energy photon beams, of EDBreast Fricke gel with MRI readings led to a dosimetry method that is suitable for the evaluation of dose distributions in the range 2 – 20 Gy, with about 8 % uncertainty on the dose measured for a 20 Gy irradiation dose. Its composition, with its high sucrose concentration, has the advantage of making it more sensitive at low doses than other conventional Fricke gels, and of reducing diffusion effects to a level close to Fricke gels doped with Xylenol Orange. However, its polynomial dose-response implies that the sensitivity tends to decrease for high doses, and induces the necessity of systematically establishing a calibration curve, even for measuring a relative dose distribution. As the reproducibility of the response from a preparation to another is estimated about 7 %, and the sensitivity is not stable over time, this calibration has to be done for every batch of gel approximately at the same time as the dose distribution measurements.

Profile measurements showed that the application of correction factors for diffusion effects was not reliable, and that the spatial resolution of the MRI measurements has to take into account these effects considering the dose gradients involved in the irradiation plan evaluated. With the measurements undertaken in this work, pixels of at least 1.5 mm^2 should have been chosen, and good results were obtained using gamma-index analysis with (2%/2mm) passing criteria.

Acknowledgements:
The authors would like to thank Rose-Marie Dubuisson and the 1.5 T MRI platform for their help with MRI reading (CNRS, Université Paris-Saclay, CEA, partly supported by « France Life Imaging (FLI), grant ANR-11-INBS-0006 »), Marion Baumann and Sylvain Bondiguel (CEA, Gif-sur-Yvette) for undertaking the measurements with the microDiamond detector, Jérémy Coulaud (Caelimp, Labège) and the SIMAD (Université Paul Sabatier, Toulouse) for sharing their gel composition and for their help on the chemical aspects.

Funding sources:
This work was partly funded by the French metrology institute (LNE). It was also part of 15HLT08 MRgRT and 18 NRM02 PRISM-eBT projects, which have received funding from the EMPIR programme co-financed by the Participating States and from the European Union's Horizon 2020 research and innovation programme.

References:

[1] Baldock C. Historical overview of the development of gel dosimetry: Another personal perspective. J Phys: Conf Ser 2009;164:012002. https://doi.org/10.1088/1742-6596/164/1/012002.

[2] Fricke H. The Reduction of Oxygen to Hydrogen Peroxide by the Irradiation of Its Aqueous Solution with X-Rays. J Chem Phys 1934;2:556–7. https://doi.org/10.1063/1.1749529.

[3] De Deene Y. Fundamentals of MRI measurements for gel dosimetry. J Phys: Conf Ser 2004;3:87–114. https://doi.org/10.1088/1742-6596/3/1/009.

[4] Schreiner LJ. Review of Fricke gel dosimeters. J Phys: Conf Ser 2004;3:9–21. https://doi.org/10.1088/1742-6596/3/1/003.

[5] Balcom BJ, Lees TJ, Sharp AR, Kulkarni NS, Wagner GS. Diffusion in Fe(II/III) radiation dosimetry gels measured by magnetic resonance imaging. Phys Med Biol 1995;40:1665–76. https://doi.org/10.1088/0031-9155/40/10/008.

[6] Coulaud J, Stien C, Gonneau E, Fiallo M, Brumas V, Sharrock P. A new spectroscopic method for measuring ferric diffusion coefficient in gelatin-based dosimeter gels. Biomed Phys Eng Express 2019;5:065028. https://doi.org/10.1088/2057-1976/ab50ce.

[7] Saur S, Strickert T, Wasboe E, Frengen J. Fricke gel as a tool for dose distribution verification: optimization and characterization. Phys Med Biol 2005;50:5251–61. https://doi.org/10.1088/0031-9155/50/22/003.

[8] Schulz RJ, deGuzman AF, Nguyen DB, Gore JC. Dose-response curves for Fricke-infused agarose gels as obtained by nuclear magnetic resonance. Phys Med Biol 1990;35:1611–22. https://doi.org/10.1088/0031-9155/35/12/002.

[9] Kelly RG, Jordan KJ, Battista JJ. Optical CT reconstruction of 3D dose distributions using the ferrous–benzoic–xylenol (FBX) gel dosimeter. Medical Physics 1998;25:1741–50. https://doi.org/10.1118/1.598356.

[10] Šolc J, Spěváček V. New 3D radiochromic gel dosimeters with inhibited diffusion. J Phys: Conf Ser 2009;164:012047. https://doi.org/10.1088/1742-6596/164/1/012047.

[11] Collura G, Gallo S, Tranchina L, Abbate BF, Bartolotta A, d'Errico F, et al. Analysis of the response of PVA-GTA Fricke-gel dosimeters with clinical magnetic resonance imaging. Nucl Instrum Methods Phys Res B 2018;414:146–53. https://doi.org/10.1016/j.nimb.2017.06.012.

[12] Chu KC, Jordan KJ, Battista JJ, Dyk JV, Rutt BK. Polyvinyl alcohol-Fricke hydrogel and cryogel: two new gel dosimetry systems with low Fe3 diffusion. Phys Med Biol 2000;45:955–69. https://doi.org/10.1088/0031-9155/45/4/311.

[13] Coulaud J, Brumas V, Sharrock P, Fiallo M. 3D optical detection in radiodosimetry: EasyDosit hydrogel characterization. Spectrochim Acta A Mol Biomol Spectrosc 2019;220:117124. https://doi.org/10.1016/j.saa.2019.05.029.

[14] Coulaud J, Brumas V, Fiallo M, Sharrock P, Gonneau E, Courbon F, et al. Tissue-inspired phantoms: a new range of equivalent tissue simulating breast, cortical bone and lung tissue. Biomed Phys Eng Express 2018;4:035017. https://doi.org/10.1088/2057-1976/aaac68.

[15] Healy BJ, Zahmatkesh MH, Nitschke KN, Baldock C. Effect of saccharide additives on response of ferrous-agarose-xylenol orange radiotherapy gel dosimeters. Med Phys 2003;30:2282–91. https://doi.org/10.1118/1.1597771.

[16] ISO/BIPM. JCGM 200:2012 - International vocabulary of metrology - Basic and general concepts and associated terms (VIM), 3rd edition 2012.

[17] Andreo P, Burns D, Hohlfeld K, Huq MS, Kanai T. TRS 398 - Absorbed Dose Determination in External Beam Radiotherapy: An International Code of Practice for Dosimetry based on Standards of Absorbed Dose to Water 2000.

[18] Delaunay F, Gouriou J, Daures J, Le Roy M, Ostrowsky A, Rapp B, et al. New standards of absorbed dose to water under reference conditions by graphite calorimetry for ^{60} Co and high-energy x-rays at LNE-LNHB. Metrologia 2014;51:552–62. https://doi.org/10.1088/0026-1394/51/5/552.

[19] Baldock C, Lepage M, Bäck SAJ, Murry PJ, Jayasekera PM, Porter D, et al. Dose resolution in radiotherapy polymer gel dosimetry: effect of echo spacing in MRI pulse sequence. Phys Med Biol 2001;46:449–60. https://doi.org/10.1088/0031-9155/46/2/312.

[20] Palmans H, Andreo P, Huq MS, Seuntjens J, Christaki K. TRS 483 - Dosimetry of Small Static Fields used in External Beam Radiotherapy: An IAEA–AAPM International Code of Practice for Reference and Relative Dose Determination 2017.
[21] Rogers DWO, Walters B, Kawrakow I. BEAMnrc Users Manual 2018.
[22] Rogers DWO, Kawrakow I, Seuntjens JP, Walters BRB, Mainegra-Hing E. NRC User Codes for EGSnrc 2018:97.
[23] Wendling M, Zijp LJ, McDermott LN, Smit EJ, Sonke J-J, Mijnheer BJ, et al. A fast algorithm for gamma evaluation in 3D. Med Phys 2007;34:1647–54. https://doi.org/10.1118/1.2721657.
[24] Prasad PV, Nalcioglu O, Rabbani B. Measurement of Three-Dimensional Radiation Dose Distributions Using MRI. Radiat Res 1991;128:1–13. https://doi.org/10.2307/3578060.
[25] Marrale M, Brai M, Gagliardo C, Gallo S, Longo A, Tranchina L, et al. Correlation between ferrous ammonium sulfate concentration, sensitivity and stability of Fricke gel dosimeters exposed to clinical X-ray beams. Nucl Instrum Methods Phys Res B 2014;335:54–60. https://doi.org/10.1016/j.nimb.2014.05.012.
[26] Olsson LE, Appleby A, Sommer J. A new dosimeter based on ferrous sulphate solution and agarose gel. Appl Radiat Isot 1991;42:1081–6. https://doi.org/10.1016/0883-2889(91)90015-S.
[27] Duzenli C, Sloboda R, Robinson D. A spin-spin relaxation rate investigation of the gelatin ferrous sulphate NMR dosimeter. Phys Med Biol 1994;39:1577. https://doi.org/10.1088/0031-9155/39/10/005.
[28] Hill B, Bäck SÅJ, Lepage M, Simpson J, Healy B, Baldock C. Investigation and analysis of ferrous sulfate polyvinyl alcohol (PVA) gel dosimeter. Phys Med Biol 2002;47:4233. https://doi.org/10.1088/0031-9155/47/23/309.
[29] ISO/BIPM. Guide to the Expression of Uncertainty in Measurement (GUM) 2020. https://www.bipm.org/en/publications/guides/gum.html (accessed June 11, 2020).
[30] Bero M, Zahili M. Radiochromic Gel dosimeter (FXG) chemical yield determination for dose measurements standardization. J Phys: Conf Ser 2009;164:012011. https://doi.org/10.1088/1742-6596/164/1/012011.
[31] De Deene Y. On the accuracy and precision of gel dosimetry. J Phys: Conf Ser 2007;56:72. https://doi.org/10.1088/1742-6596/56/1/007.
[32] Gustavsson H, Bäck S \AA J, Lepage M, Rintoul L, Baldock C. Development and optimization of a 2-hydroxyethylacrylate MRI polymer gel dosimeter. Phys Med Biol 2004;49:227–41. https://doi.org/10.1088/0031-9155/49/2/004.
[33] Lepage M. Magnetic resonance in polymer gel dosimetry: Techniques and optimization. J Phys: Conf Ser 2006;56:86–94. https://doi.org/10.1088/1742-6596/56/1/008.
[34] Trapp JV, Bäck SAJ, Lepage M, Michael G, Baldock C. An experimental study of the dose response of polymer gel dosimeters imaged with x-ray computed tomography. Phys Med Biol 2001;46:2939–51. https://doi.org/10.1088/0031-9155/46/11/312.
[35] Venning AJ, Hill B, Brindha S, Healy BJ, Baldock C. Investigation of the PAGAT polymer gel dosimeter using magnetic resonance imaging. Phys Med Biol 2005;50:3875–88. https://doi.org/10.1088/0031-9155/50/16/015.
[36] Vergote K, De Deene Y, Duthoy W, Gersem WD, Neve WD, Achten E, et al. Validation and application of polymer gel dosimetry for the dose verification of an intensity-modulated arc therapy (IMAT) treatment. Phys Med Biol 2004;49:287–305. https://doi.org/10.1088/0031-9155/49/2/008.
[37] Cho N-Y, Huang S-C, Chung W-Y, Guo W-Y, Chu W-C. Isotropic three-dimensional MRI-Fricke-infused gel dosimetry. Med Phys 2013;40:052101. https://doi.org/10.1118/1.4798228.
[38] Viti V, d'Errico F, Pacilio M, Luciani AM, Palma A, Grande S, et al. Optical imaging of dose distributions in Fricke gels. Radiat Prot Dosimetry 2006;120:148–50. https://doi.org/10.1093/rpd/ncj005.
[39] Rousseau A, Stien C, Bordy J-M, Blideanu V. Fricke-Xylenol orange-Gelatin gel characterization with dual wavelength cone-beam optical CT scanner for applications in stereotactic and dynamic radiotherapy. Phys Med 2022;97:1–12. https://doi.org/10.1016/j.ejmp.2022.03.008.
[40] Olsson LE, Petersson S, Ahlgren L, Mattsson S. Ferrous sulphate gels for determination of absorbed dose distributions using MRI technique: basic studies. Phys Med Biol 1989;34:43–52. https://doi.org/10.1088/0031-9155/34/1/004.

[41] ICRU. Measurement of low-level radioactivity ICRU Report 22, issued by the International Commission on Radiation Units and Measurements 1972.
[42] Davies JB, Baldock C. Sensitivity and stability of the Fricke–gelatin–xylenol orange gel dosimeter. Radiat Phys Chem 2008;77:690–6. https://doi.org/10.1016/j.radphyschem.2008.01.007.
[43] Marini A, Lazzeri L, Cascone MG, Ciolini R, Tana L, d'Errico F. Fricke gel dosimeters with low-diffusion and high-sensitivity based on a chemically cross-linked PVA matrix. Radiat Meas 2017;106:618–21. https://doi.org/10.1016/j.radmeas.2017.02.012.
[44] Bero MA, Gilboy WB, Glover PM, Keddie JL. Three-dimensional radiation dose measurements with Ferrous Benzoic Acid Xylenol Orange in Gelatin gel and optical absorption tomography. Nucl Instrum Methods Phys Res A 1999;422:617–20. https://doi.org/10.1016/S0168-9002(98)00970-X.
[45] Del Lama LS, Petchevist PCD, de Almeida A. Fricke Xylenol Gel characterization at megavoltage radiation energy. Nucl Instrum Methods Phys Res B 2017;394:89–96. https://doi.org/10.1016/j.nimb.2016.12.045.
[46] Bero MA, Gilboy WB, Glover PM. Radiochromic gel dosemeter for three-dimensional dosimetry. Radiat Phys Chem 2001;61:433–5. https://doi.org/10.1016/S0969-806X(01)00289-4.
[47] Low DA, Harms WB, Mutic S, Purdy JA. A technique for the quantitative evaluation of dose distributions. Med Phys 1998;25:656–61. https://doi.org/10.1118/1.598248.
[48] MacDougall ND, Miquel ME, Keevil SF. Effects of phantom volume and shape on the accuracy of MRI BANG gel dosimetry using BANG3TM. BJR 2008;81:46–50. https://doi.org/10.1259/bjr/71353258.
[49] De Deene Y, Vandecasteele J. On the reliability of 3D gel dosimetry. J Phys: Conf Ser 2013;444:012015. https://doi.org/10.1088/1742-6596/444/1/012015.
[50] Mann P, Schwahofer A, Karger CP. Absolute dosimetry with polymer gels—a TLD reference system. Phys Med Biol 2019;64:045010. https://doi.org/10.1088/1361-6560/aafd41.
[51] Xu Y, Wuu C-S, Maryanski MJ. Sensitivity calibration procedures in optical-CT scanning of BANG 3 polymer gel dosimeters. Med Phys 2010;37:861–8. https://doi.org/10.1118/1.3298017.
[52] Awad SI, Moftah B, Basfer A, Almousa AA, Al Kafi MA, Eyadeh MM, et al. 3-D Quality Assurance in CyberKnife Radiotherapy Using a Novel N-(3-methoxypropyl) Acrylamide Polymer Gel Dosimeter and Optical CT. Radiat Phys Chem 2019;161:34–41. https://doi.org/10.1016/j.radphyschem.2019.03.045.
[53] Oldham M, Baustert I, Lord C, Smith TAD, McJury M, Warrington AP, et al. An investigation into the dosimetry of a nine-field tomotherapy irradiation using BANG-gel dosimetry. Phys Med Biol 1998;43:1113–32. https://doi.org/10.1088/0031-9155/43/5/005.
[54] Colnot J, Huet C, Gschwind R, Clairand I. Characterisation of two new radiochromic gel dosimeters TruView^{TM} and ClearView^{TM} in combination with the vista^{TM} optical CT scanner: A feasibility study. Phy Med 2018;52:154–64. https://doi.org/10.1016/j.ejmp.2018.07.002.
[55] Babic S, Battista J, Jordan K. Three-Dimensional Dose Verification for Intensity-Modulated Radiation Therapy in the Radiological Physics Centre Head-and-Neck Phantom Using Optical Computed Tomography Scans of Ferrous Xylenol–Orange Gel Dosimeters. Int J Radiat Oncol Biol Phys 2008;70:1281–91. https://doi.org/10.1016/j.ijrobp.2007.11.032.
[56] Oldham M, McJury M, Baustert IB, Webb S, Leach MO. Improving calibration accuracy in gel dosimetry. Phys Med Biol 1998;43:2709–20. https://doi.org/10.1088/0031-9155/43/10/002.
[57] Oldham M, Siewerdsen J, Shetty A, Jaffray D. High resolution gel-dosimetry by optical-CT and MR scanning. Med Phys 2001;28:1436–45. https://doi.org/10.1118/1.1380430.
[58] Oldham M, Siewerdsen JH, Kumar S, Wong J, Jaffray DA. Optical-CT Gel-Dosimetry I: Basic Investigations. Med Phys 2003;30:623–34. https://doi.org/10.1118/1.1559835.
[59] Oldham M. Methods and techniques for comprehensive 3D dosimetry. Advances in Medical Physics, 5 ed D J Godfrey et al.; 2014.
[60] Smith ST, Masters KS, Hosokawa K, Blinco J, Crowe SB, Kairn T, et al. A reduction of diffusion in PVA Fricke hydrogels. J Phys: Conf Ser 2015;573:012046. https://doi.org/10.1088/1742-6596/573/1/012046.

[61] Lazzeri L, Marini A, Cascone MG, d'Errico F. Dosimetric and chemical characteristics of Fricke gels based on PVA matrices cross-linked with glutaraldehyde. Phys Med Biol 2019;64:085015. https://doi.org/10.1088/1361-6560/ab135c.
[62] Coulaud J. Sécurisation des traitements radiothérapeutiques du cancer : validation physique des plans théoriques de radiothérapie par des fantômes dosimétriques anthropomorphes. These de doctorat. Toulouse 3, 2020.